Pore pressure and poroelasticity effects in Coulomb stress analysis of earthquake interactions

Massimo Cocco

Istituto Nazionale di Geofisica e Vulcanologia, Rome, Italy

James R. Rice

Engineering Sciences and Geophysics, Harvard University, Cambridge, Massachusetts, USA

[1] Pore pressure changes are rigorously included in Coulomb stress calculations for fault interaction studies. These are considered changes under undrained conditions for analyzing very short term postseismic response. The assumption that pore pressure is proportional to fault-normal stress leads to the widely used concept of an effective friction coefficient. We provide an exact expression for undrained fault zone pore pressure changes to evaluate the validity of that concept. A narrow fault zone is considered whose poroelastic parameters are different from those in the surrounding medium, which is assumed to be elastically isotropic. We use conditions for mechanical equilibrium of stress and geometric compatibility of strain to express the effective normal stress change within the fault as a weighted linear combination of mean stress and fault-normal stress changes in the surroundings. Pore pressure changes are determined by fault-normal stress changes when the shear modulus within the fault zone is significantly smaller than in the surroundings but by mean stress changes when the elastic mismatch is small. We also consider an anisotropic fault zone, introducing a Skempton tensor for pore pressure changes. If the anisotropy is extreme, such that fluid pressurization under constant stress would cause expansion only in the fault-normal direction, then the effective friction coefficient concept applies exactly. We finally consider moderately longer timescales than those for undrained response. A sufficiently permeable fault may come to local pressure equilibrium with its surroundings even while that surrounding region may still be undrained, leading to pore pressure change determined by mean stress changes in those surroundings. *INDEX TERMS:* 7209 Seismology: Earthquake dynamics and mechanics, 7260 Seismology: Theory and modeling, 7215 Seismology: Earthquake parameters; *KEYWORDS:* Fault interaction, fluid flow, poroelasticity, effective friction, crustal anisotropy

1. Introduction

[2] Earthquakes produce changes in the state of strain and stress in the volume surrounding the causative faults. Coseismic stress and strain changes caused by shear dislocations are usually calculated using the numerical procedure proposed by *Okada* [1985, 1992]. This approach is based on the solution of the elastostatic equations in an elastic, isotropic homogeneous half-space. The coseismic strain and stress fields can be computed if the geometry and the slip distribution on the rupturing fault plane are known (see *Okada* [1992], *Stein et al.* [1992], *King et al.* [1994], *Stein* [1999], and *King and Cocco* [2000], among several others). In the near field the induced coseismic stress consists both of a dynamic (transient) and a static (permanent) perturbation. The calculation of dynamic stress changes requires the solution of the elastodynamic equations. It implies that both shear and fault-normal stresses can vary as functions of times reaching the static configuration after a few tens of seconds [*Harris and Day*, 1993; *Cotton and Coutant*, 1997; *Belardinelli et al.*, 1999, and references therein].

[3] Fault interaction is currently investigated by means of these analytical formulations and using the induced stress on a specified fault plane to compute Coulomb stress changes. In the framework of the Coulomb criterion, failure on a fault occurs when the applied stress increment, defined as

$$\Delta CFF = \Delta\tau + \mu(\Delta\sigma + \Delta p), \qquad (1)$$

overcomes a stress threshold, where $\Delta\tau$ is the shear stress change (computed in the slip direction), $\Delta\sigma$ is the fault-normal stress change (positive for extension), Δp is the pore pressure change within the fault, and μ is the friction coefficient which ranges between 0.6 and 0.8 for most rocks [see *Harris*, 1998, and references therein]. The quantities included in (1) should be considered as functions of time.

[4] Earthquakes perturb the state of stress of a crustal volume, and they cause a variety of hydrologic phenomena [*Scholz*, 1990; *Sibson*, 1994; *King and Muir-Wood*, 1994; *Roeloffs*, 1996, 1998; *Roeloffs and Quilty*, 1997]. Some of these effects can be explained by the poroelastic response to the earthquake-induced strain field. Pore pressure changes modify the coseismic stress redistribution, and for this reason they are included in the definition of the Coulomb failure function (1). Because the coseismic stress changes occur on a timescale that is too short to allow the loss or gain of pore fluid by diffusive transport (fluid flow), the pore pressure changes included in (1) on that timescale are associated with the undrained response of the medium [*Rice and Cleary*, 1976]. Later, we discuss somewhat longer timescales for which the fault is no

longer undrained. The undrained conditions are those for which there is no fluid flow. From an analytical point of view the undrained response implies that the fluid mass content per unit volume is constant ($\Delta m = 0$), but the pore pressure is altered. Under these conditions the relationship between stress and strain for a fluid-infiltrated poroelastic material is equivalent to an ordinary elastic material with appropriate coefficients for the undrained conditions [*Rice and Cleary*, 1976; *Roeloffs*, 1996].

[5] According to *Rice and Cleary* [1976] the pore pressure change resulting from a change in stress under undrained conditions is given by

$$\Delta p = -B \frac{\Delta \sigma_{kk}}{3}, \tag{2}$$

where B is the Skempton coefficient [*Skempton*, 1954; *Kuempel*, 1991]. *Rice and Cleary* [1976], *Roeloffs and Rudnicki* [1985], and *Roeloffs* [1996] present a compilation of experimental determinations of B indicating a range between 0.5 and 0.9. In Coulomb stress analysis [see *Stein et al.*, 1992; *Harris and Simpson*, 1992; *King et al.*, 1994; *Harris*, 1998, and references therein] it is assumed that for plausible fault zone rheologies the change in pore pressure becomes proportional to the fault-normal stress:

$$\Delta p = -\hat{B} \Delta \sigma. \tag{3}$$

This is certainly true if in the fault zone $\Delta \sigma_{11} = \Delta \sigma_{22} = \Delta \sigma_{33}$, so that $\Delta \sigma_{kk}/3 = \Delta \sigma$ and (2) becomes (3) [see *Simpson and Reasenberg*, 1994; *Harris*, 1998]. By substituting (3) in (1), we obtain

$$\Delta \text{CFF} = \Delta \tau + \mu' \Delta \sigma, \tag{4}$$

where $\mu' = \mu(1 - \hat{B})$ is the effective (or apparent) friction coefficient. Equation (4) is very common in the literature, and it has been widely used to calculate Coulomb stress changes [see *Harris*, 1998, and references therein]. A variety of values are used for these calculations: the friction coefficient μ ranges between 0.6 and 0.8, while B ranges between 0.5 and 1 [*Green and Wang*, 1986; *Hart*, 1994]. The resulting values for the effective friction coefficient range between 0.0 and 0.75 (0.4 has been used in many calculations by *Stein et al.* [1992] and *King et al.* [1994]). Several studies have concluded that Coulomb stress modeling is only modestly dependent on the assumed value of the effective friction coefficient [see *King et al.*, 1994]. This result might depend on the choice of the poroelastic model (equation (2) or (3)) in Coulomb stress analyses. It is important to emphasize that the effective friction coefficient μ' is not a material property, but it depends on the ratios of stress changes in the medium [*Byerlee*, 1992; *Hill et al.*, 1993; *Beeler et al.*, 2000].

[6] Several recent papers have focused attention on the correlation between fault-normal stress changes and earthquake locations as well as seismicity rate changes [see *Perfettini et al.*, 1999; *Parsons et al.*, 1999; *Cocco et al.*, 2000, and references therein]. However, it is still not well understood why these fault-normal stress changes should provide a better explanation of this correlation than Coulomb stresses. Fluid flow (time-dependent) as well as the choice of the proper expression for Δp in Coulomb analyses might help to explain some aspects of this paradox.

[7] *Beeler et al.* [2000] pointed out that using the constant apparent friction model (equation (4)) in Coulomb analyses may provide a misleading view in estimating stress changes. They compare that model with an isotropic and homogeneous (same properties within the fault as outside) poroelastic model, equations (1) and (2), and conclude that Coulomb failure stress shows considerable differences for different tectonic environments. It is important to emphasize that because of fluid flow the induced pore

pressure changes are time-dependent; therefore it is necessary to specify the timescale during which the poroelastic model is applied.

[8] This paper discusses the assumptions required to correctly include the pore pressure changes in Coulomb stress modeling and provides a more general expression for the effective normal stress for different timescales. We start investigating the short-term postseismic period, in which both the fault zone and the adjoining lithosphere respond under undrained conditions. In this case we first assume that the fault zone is a poroelastic isotropic medium, but we will also consider the effect of anisotropy within the fault zone. Then we study an intermediate timescale, which will exist for a sufficiently permeable fault, during which the fault core reaches a local pressure equilibrium with its lithospheric surroundings, while the adjoining lithosphere is still responding as if it were undrained. We will not consider here longer timescales during which the transition from short-term undrained response to long-term drained response takes place also in the surrounding lithosphere.

2. Poroelastic Constitutive Relations

[9] The stress-strain relation for an ordinary isotropic linearly elastic solid can be expressed as

$$2G\varepsilon_{ij} = \sigma_{ij} - \frac{\lambda}{3\lambda + 2G}\sigma_{kk}\delta_{ij}, \tag{5}$$

where ε_{ij} and σ_{ij} are the strain and stress tensors, respectively; G and λ are the Lamé parameters (G is the rigidity) and δ_{ij} is the Kronecker delta. Hooke's law (5) can be rewritten using the Poisson ratio v●● as

$$2G\varepsilon_{ij} = \sigma_{ij} - \frac{v}{1+v}\sigma_{kk}\delta_{ij}. \tag{6}$$
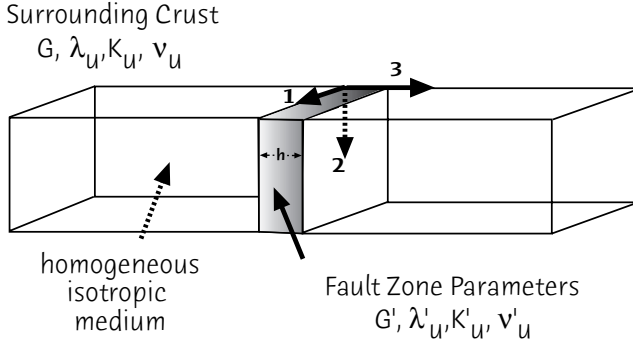
Because here we consider linear elasticity, these constitutive relations must be applied to small stress-strain magnitudes. We assume that they are valid in such isotropic form for coseismic stress-strain changes caused by shear dislocations, which are of interest since we do not know the absolute value of the regional remote tectonic stress.

[10] Because compact rocks consisting of solid phase materials are not an appropriate model for the crust, we have to consider our medium as porous or cracked. The stress-strain relations for a poroelastic medium are slightly different from (6) because they include the pore pressure term [*Biot*, 1941, 1956; *Rice and Cleary*, 1976]. According to *Rice and Cleary* [1976], these constitutive relations are

$$2G\varepsilon_{ij} = \sigma_{ij} - \frac{v}{1+v}\sigma_{kk}\delta_{ij} + \frac{3(v_u - v)}{B(1+v)(1+v_u)}p\delta_{ij} \tag{7a}$$

$$m = m_0 + \frac{3\rho_0(v_u - v)}{2GB(1+v)(1+v_u)}\left(\sigma_{kk} + \frac{3}{B}p\right), \tag{7b}$$

where m_0, ρ_0 are the fluid mass content and the density measured with respect to a reference state at which we take $P = 0$. Here v is the Poisson ratio under drained conditions, whereas the term v_u represents the undrained Poisson ratio, which is a function of v, the bulk modulus (K), and the Skempton coefficient (B) of the medium [see *Rice and Cleary*, 1976; *Kuempel*, 1991]. Equation (7b) shows that for undrained conditions ($\Delta m = 0$), $\Delta p = -B\Delta\sigma_{kk}/3$ yielding (2) when pore pressure and mean stress changes are considered. Equation (7a) is equivalent to (6) for a poroelastic medium if v in (6) is replaced by v_u. In fact, using the relation (2) in (7a) to

Surrounding Crust
G, λ_u, K_u, ν_u

homogeneous
isotropic
medium

Fault Zone Parameters
$G', \lambda'_u, K'_u, \nu'_u$

Figure 1. Undrained poroelastic fault model.

describe undrained (e.g., coseismic) strain and stress changes, we get the following constitutive relation:

$$2G\Delta\varepsilon_{ij} = \Delta\sigma_{ij} - \frac{\nu_u}{1+\nu_u}\Delta\sigma_{kk}\delta_{ij}. \tag{8}$$

Equation (8) is equivalent to (6) but now represents a poroelastic medium under undrained conditions.

[11] The following relation [*Rice and Cleary*, 1976] relates the undrained Poisson ratio to the other poroelastic parameters:

$$\nu_u = \frac{3\nu + B(1-2\nu)\left(1-\frac{K}{K_s}\right)}{3 - B(1-2\nu)\left(1-\frac{K}{K_s}\right)}, \tag{9}$$

where K is the bulk modulus of the saturated rock under drained conditions and K_s is a modulus which, for certain simple materials (uniform properties of solid phase in response to hydrostatic stressing, fully interconnected pore space), can be equated to the bulk modulus of the solid grains in the rock. We emphasize that if $K = K_s$, then $\nu_u = \nu$. In general, the undrained bulk modulus is larger than the drained one, and $K_s > K_u > K$. According to (9) the undrained Poisson ratio is larger than the drained Poisson ratio ($\nu_u > \nu$). The same is true for the Lamé parameter, $\lambda_u > \lambda$. The rigidity, on the contrary, remains the same, $G_u = G$. These considerations suggest that the fault stiffness for undrained conditions is larger than that for drained ones.

3. Pore Pressure Changes in an Undrained Poroelastic Fault Model

[12] We investigate the stress conditions for a fault in a poroelastic medium. The fault zone materials have different properties with respect to the surroundings. Let 1 and 2 represent the coordinate directions in the fault zone and 3 represent the coordinate direction perpendicular to the fault plane (Figure 1). The stress-strain relations for the medium are given by (8). We interpret the elastic moduli here as moduli for undrained deformation. We indicate with G', λ'_u, K'_u, ν'_u the Lamé and bulk moduli and the Poisson ratio within the fault zone, while G, λ_u, K_u, ν_u denote the parameters in the surrounding crust. In the following, we use the stress-strain relation for a poroelastic medium in the form of (5), using the Lamé moduli.

[13] Considering the conditions of mechanical equilibrium and strain compatibility, there exist equality conditions for strain and stress components within the fault zone and outside it, in the cases that we consider here, for which fault zone thickness is much less than length scales over which stress and strain vary outside the fault. We indicate with ε_{ij}' and σ_{ij}' ●the strain and the stress tensors within the fault zone. Kinematic compatibility implies that certain

strain components are the same inside and outside the fault zone [*Rice*, 1992], namely, $\varepsilon_{11}' = \varepsilon_{11}$, $\varepsilon_{22}' = \varepsilon_{22}$, $\varepsilon_{12}' = \varepsilon_{12}$. Similarly, conditions of mechanical equilibrium require that certain stress components must be the same everywhere within the fault zone as in the nearby crust outside it, namely, $\sigma_{33}' = \sigma_{33}$, $\sigma_{31}' = \sigma_{31}$, $\sigma_{32}' = \sigma_{32}$. In other words, the equilibrium conditions on the problem restrict σ_{33} ●to continuity but leave the other normal components unrestricted. This means that the other stress components inside the fault zone may be different from those outside it. They are determined from mechanical constitutive relations.

[14] According to (5) we have the following relations:

$$2(\varepsilon_{11} + \varepsilon_{22}) = \frac{1}{G}\left[\sigma_{11} + \sigma_{22} - \frac{2\lambda_u}{3\lambda_u + 2G}\sigma_{kk}\right] \tag{10a}$$

$$2(\varepsilon_{11}' + \varepsilon_{22}') = \frac{1}{G'}\left[\sigma_{11}' + \sigma_{22}' - \frac{2\lambda_u'}{3\lambda_u' + 2G'}\sigma_{kk}'\right], \tag{10b}$$

where primes denote quantities inside the fault zone. Using the continuity conditions for the strain components appearing in (10a) and (10b) and for the fault-normal stress, we can write

$$\frac{1}{G}\left[\frac{\lambda_u + 2G}{3\lambda_u + 2G}\sigma_{kk} - \sigma_{33}\right] = \frac{1}{G'}\left[\frac{\lambda_u' + 2G}{3\lambda_u' + 2G'}\sigma_{kk}' - \sigma_{33}\right]. \tag{11}$$

[15] For a slightly more concise notation, let $M = \lambda + 2G$ be the modulus for one-dimensional strain and recall that $K = \lambda + 2G/3$. Then (11) becomes

$$\frac{1}{G}\left[\frac{M_u}{K_u}\frac{\sigma_{kk}}{3} - \sigma_{33}\right] = \frac{1}{G'}\left[\frac{M_u'}{K_u'}\frac{\sigma_{kk}'}{3} - \sigma_{33}\right],$$

where the quantity M_u/K_u corresponds to $(1 - \nu_u)/(1 + \nu_u)$, which might be alternatively used in the following equations (with primes denoting the values within the fault zone). Solving the previous relation for $\sigma_{kk}'/3$ within the fault zone, we get

$$\frac{\sigma_{kk}'}{3} = \frac{K_u'}{M_u'}\left[\frac{G'}{G}\frac{M_u}{K_u}\frac{\sigma_{kk}}{3} + \frac{G - G'}{G}\sigma_{33}\right]. \tag{12a}$$

To emphasize that this applies for the stress changes caused by a nearby earthquake, we write

$$\frac{\Delta\sigma_{kk}'}{3} = \frac{K_u'}{M_u'}\left[\frac{G'}{G}\frac{M_u}{K_u}\frac{\Delta\sigma_{kk}}{3} + \frac{G - G'}{G}\Delta\sigma_{33}\right] \tag{12b}$$

and understand the unprimed stress changes ($\Delta\sigma_{ij}$) to be those conventionally computed by elastic dislocation theory. For Coulomb analysis we need to know the pore pressure changes induced in the fault zone, which we obtain by substituting (12b) in (2):

$$\Delta p' = -B'\frac{\Delta\sigma_{kk}'}{3} = -B'\frac{K_u'}{M_u'}\left[\frac{G'}{G}\frac{M_u}{K_u}\frac{\Delta\sigma_{kk}}{3} + \frac{G - G'}{G}\Delta\sigma_{33}\right], \tag{13}$$

where B' is the Skempton coefficient in that fault zone. Equation (13) shows that induced pore pressure changes depend both on the mean stress and the fault-normal stress changes. The relevant effective normal stress change for Coulomb stress analysis is thus

$$\Delta\sigma_{33}^{\text{eff}} = \Delta\sigma_{33}' + \Delta p' = \Delta\sigma_{33} - B'\frac{\Delta\sigma_{kk}'}{3}$$

$$= \Delta\sigma_{33} - B'\frac{K_u'}{M_u'}\left[\frac{G'}{G}\frac{M_u}{K_u}\frac{\Delta\sigma_{kk}}{3} + \frac{G - G'}{G}\Delta\sigma_{33}\right]. \tag{14}$$

[16] Equations (13) and (14) give the relative weights of fault-normal and mean stress perturbations in determining the pore pressure and Coulomb stress changes. In general, the pore pressure changes depend on both these quantities. In particular, the pore pressure changes are related to the fault-normal stress changes through the rigidity contrast between fault zone materials and the surrounding crust.

[17] We can recognize two limiting cases for (14). The first one holds when $G' = G$ and the mean stress is the relevant quantity. Thus (14) becomes

$$\Delta\sigma_{33}^{\text{eff}} = \Delta\sigma_{33} - B'\frac{K'_u}{K_u}\frac{M_u}{M'_u}\frac{\Delta\sigma_{kk}}{3}, \quad (15)$$

the second limiting case is obtained when $G \gg G'$, and (14) becomes

$$\Delta\sigma_{33}^{\text{eff}} = \left(1 - B'\frac{K'_u}{M'_u}\right)\Delta\sigma_{33}. \quad (16)$$

[18] Equations (15) and (16) express the effective normal stress changes for the case where pore pressure changes depend solely on mean or fault-normal stress changes, respectively. Equation (16) is equivalent to the effective friction approach of (4) if the Skempton parameter is given by $\hat{B} = B'K'_u/M'_u$.

4. Elastic Moduli in the Fault Zone

[19] Equation (13) relates pore pressure changes to fault-normal and mean stress changes through two factors, which depend on the elastic parameters in the fault zone and in the surrounding crust. The variation of these elastic parameters is reflected in the variation of P and S wave velocities. Therefore information on shear wave velocity anomalies in the fault zone might be used to constrain numerical values of the factors appearing in (13) and to discuss the two limiting cases reported in (15) and (16). In particular, the following relations hold (assuming that measured P wave speeds correspond approximately to undrained response in the sense of poroelasticity):

$$\frac{M_u}{G} = \left(\frac{V_P}{V_S}\right)^2 ; K_u = G\left(\frac{M_u}{G} - 43\right) = G\left(\frac{V_P^2}{V_S^2} - \frac{4}{3}\right), \quad (17)$$

and the same relations with primes (K'_u, M'_u) indicate the moduli inside the fault zone. This equation yields

$$\frac{K_u}{M_u} = 1 - \frac{4}{3}\left(\frac{V_S}{V_P}\right)^2 \quad (18)$$

for the quantity which appears in (14). The square of the S wave velocity anomaly of the fault zone with respect to the surrounding crust is related to the density and rigidity of the two media:

$$\frac{V_S^2 - V_S'^2}{V_S^2} = \frac{\rho' G - \rho G'}{\rho' G},$$

where ρ is the density. A similar relation holds for the modulus for one-dimensional strain M and the P wave velocity anomaly:

$$\frac{V_P^2 - V_P'^2}{V_P^2} = \frac{\rho' M_u - \rho M'_u}{\rho' M_u}.$$

[20] If the density contrast between the fault zone materials and the surrounding crust is not very large ($\rho \approx \rho'$), the relative variation of G and M can be expressed as

$$\frac{G - G'}{G} = \frac{\rho V_S^2 - \rho' V_S'^2}{\rho V_S^2} \approx \frac{V_S^2 - V_S'^2}{V_S^2},$$
$$\frac{G'}{G} = \left(\frac{V_S'}{V_S}\right)^2, \quad (19)$$
$$\frac{M'_u}{M_u} = \left(\frac{V_P'}{V_P}\right)^2.$$

[21] An opposite limiting case exists when the rigidity contrast is negligible (G' approximately equal to G), and therefore we have

$$\frac{V_S^2 - V_S'^2}{V_S^2} \approx \frac{\rho' - \rho}{\rho'}.$$

[22] This latter case represents the limiting case (G' approximately equal to G) yielding (15), and mean stress perturbations are the only contribution to the effective normal stress changes.

[23] In a first simplified model we assume that the fault zone is a solid of the same lithology as the adjoining crust, densely fractured with an isotropic distribution of cracks saturated by fluids, while the crust is considered as a much less cracked but still saturated Poissonian body ($\lambda = G$). We consider that none of the crack walls can open or close toward one another when an isotropic stress is applied, so they produce no change in volume and hence no alteration of K'_u. We can thus observe that the bulk modulus K'_u is unaffected by the presence of saturated cracks, at least assuming that their aspect ratio is much less than the ratio of liquid bulk modulus to solid bulk modulus, as pointed out by *O'Connell and Budiansky* [1974]. Assuming that the fault zone has the same lithology as the surroundings, just much more cracked, implies that $K'_u = K_u$. This also means that $\rho = \rho'$, neglecting the crack space contributions to volume. In these conditions the crack walls can slide in shear, so that G is reduced ($G' < G$), yielding (19).

[24] We use seismic evidence for P and S wave velocity variations to infer possible values of the elastic moduli in the fault zone. Studies of local crustal tomography provide evidence on the body wave velocity variations in fault zones. Although several studies (mostly based on V_P tomographic images) interpreted the fault zone as a high-velocity body [*Lees*, 1990; *Lees and Nicholson*, 1993; *Zhao and Kanamori*, 1993, 1995], many others have suggested the presence of fluids within the fault zone [*Eberhart-Phillips and Michael*, 1993; *Johnson and McEvilly*, 1995; *Thurber et al.*, 1997]. *Zhao et al.* [1996] and *Zhao and Negishi* [1998] found evidence of low P and S wave velocities and high Poisson ratio at the hypocenter of the 1995 Kobe earthquake. We remark that V_S and the Poisson ratio● v_u (or V_P/V_S) are much more sensitive to fluids than V_P [see also *Eberhart-Phillips and Reyners*, 1999].

[25] Studies on fault zone trapped waves yield more useful constraints to the quantities defined in (17) and (19) because they have an optimal resolution of the inner structure of fault zones whose thickness can range between 20 and 400 m [*Li et al.*, 1990, 1994]. *Li and Leary* [1990] have shown the fracture density and the S wave velocity model for the Oroville (California) fault zone as determined by body wave travel time modeling. They clearly show that the fault zone corresponds to a reduction in shear wave velocity (roughly 50%) and an increase of the crack density (up to 0.75). *Li et al.* [1990, 1994] point out that the reduction in S wave velocity inside the fault zone ranges from 30 to 50%. According to *Mooney and Ginzburg* [1986] and *Li and Leary* [1990] the velocity structure of the Calaveras fault shows a P wave velocity reduction of nearly 30%.

[26] Although our review of velocity models of fault zones is far from complete, we use these representative values to estimate the quantities defined above. According to the aforementioned studies and to relations (17), (18), and (19) if V_S'/V_S ranges between 0.5 and 0.7, the rigidity ratio G'/G ranges between 0.25 and 0.5. This implies that the rigidity reduction $(G - G')/G$ is between 0.75 and 0.5. As expected, if the reduction in S wave velocity within the fault zone is very large (50–70%) the ratio G'/G becomes much smaller than $(G - G')/G$. Moreover, if we assume that the reduction in S wave velocity is larger than that in P wave, then the V_P'/V_S' ratio inside the fault zone is larger than the corresponding value in the surrounding crust. We consider the simplified model described above, which yields $K_u' = K_u$ (= $5G/3$ in a Poissonian surrounding crust), and then given G'/G, we can calculate M_u':

$$M_u' = K_u' + \frac{4}{3}G' = K_u + \frac{4}{3}\frac{G'}{G}G = \left(\frac{5}{3} + \frac{4}{3}\frac{G'}{G}\right)G.$$

[27] This results in

$$\frac{K_u'}{M_u'} = \frac{K_u}{M_u'} = \frac{5}{3}\frac{G}{M_u'} = \frac{5}{5 + 4\frac{G'}{G}}.$$

[28] According to this relation the ratio K_u'/M_u' ranges between 0.714 and 0.883 for G'/G between 0.5 and 0.25, while it is equal to 0.556 for $G'/G = 1$. As an example, we provide a tentative estimate of the two proportionality factors that appear in (13). We assume a reduction in P and S wave velocities in the fault zone of 18% and 50%, respectively. These assumptions yield

$$\frac{G - G'}{G} = 0.75; \frac{G'}{G} = 0.25; \frac{K_u}{M_u} = 0.556; \frac{K_u'}{M_u'} = 0.883.$$

[29] Using these values, the constants which multiply the mean and the fault-normal stress changes in (13) and (14) are 0.45 and 0.75, respectively. The latter does not seem to be negligible at all, and for this illustration,

$$\Delta p' = -B'\left[0.375\frac{\Delta\sigma_{kk}}{3} + 0.625\Delta\sigma_{33}\right]$$
$$= -B'[0.125(\Delta\sigma_{11} + \Delta\sigma_{22}) + 0.750\Delta\sigma_{33}].$$

[30] Thus the assumption that $\Delta p'$ is proportional only to $\Delta\sigma_{kk}/3$ does not seem to be strongly supported by observation of P and S wave velocities, but at the same time, neglecting this term may be justifiable only if the reduction in S wave velocity is much larger than 50%, at least under the conditions assumed in the simplified model considered here. This model can be reasonable for faults that have experienced little slip, but it might be not reliable for a relatively mature fault zone. In this latter case, the presence of a fault gouge with a different porosity, and possibly fluid-altered composition, with respect to the host lithology might be more properly represented by a density contrast [*Mooney and Ginzburg*, 1986], so that $\rho' < \rho$. Even in this case, we can show that the change in the one-dimensional strain modulus M is larger than the change in density. According to *Mooney and Ginzburg* [1986] we can assume that $\Delta V_P/V_P = F\Delta\rho/\rho$, with $F \geq 1$, and write

$$\frac{\Delta V_P}{V_P} = \frac{1}{2}\left[\frac{\Delta M_u'}{M_u'} - \frac{\Delta\rho}{\rho}\right]\frac{\Delta M_u'}{M_u'} = (1 + 2F)\frac{\Delta\rho}{\rho}.$$

[31] This gives a greater change in modulus M_u' rather than in ρ so that, approximately, neglect of ρ ●changes in our estimate of modulus changes, as in (19), is still valid. Note that for a given G'/G, a different reduction from M_u to M_u' than what we have

estimated does not affect the relative importance of mean stress and fault normal stress in (13) for $\Delta p'$; it only affects the factor K_u'/M_u' in front.

5. Modeling Static Stress Changes From Shear Dislocations

[32] In this section we aim to compare the shear, fault-normal, and mean static stress changes caused either by a vertical strike-slip fault or a normal fault in an elastic homogeneous half-space. We use the three-dimensional (3-D) dislocation code developed by *Nostro et al.* [1997], which is based on numerical representation provided by *Okada* [1985, 1992]. Again, our discussion here is directed to the short timescale for which the fault and its surroundings respond as if undrained. The elastic stress changes caused by shear dislocations illustrate the spatial variability and absolute values of the different terms in (1), (2), and (4) and allow a comparison between the Coulomb stress changes resulting from the application of (1) as opposed to (4). Figure 2a shows the shear, normal, and Coulomb stress changes caused by a vertical strike-slip fault mapped both on a horizontal layer at 6 km depth as well as on a vertical cross section A-A' perpendicular to the fault strike. Coulomb stress changes have been computed by means of (4) on secondary faults having the same orientation and mechanism of the causative fault and using a constant effective friction equal to 0.4 (corresponding to $\mu = 0.75$ and $B = 0.47$). *King et al.* [1994] have already discussed these stress patterns in detail; here we only remark that positive stress changes can favor failures on appropriately oriented planes. We also point out that the variability of the stress patterns on the horizontal maps, where both s_1 and s_3 lie, is more evident for strike-slip faults than on the vertical cross sections. Moreover, the amplitudes of fault-normal stress changes at depth are quite small. It is important to remark that the cross section is not taken in the middle of the rupturing fault because such a direction is nodal for fault-normal stress changes, as shown in the map view. Figure 2b shows similar results for a normal fault dipping 70° to the east; we only show the E-W vertical cross section calculated in the middle of the fault. As expected for a normal fault, the largest spatial variability of stress changes occurs on the vertical plane used for the sections where both σ_1 and σ_3 lie.

[33] Figure 3 shows the mean stress changes caused by the vertical strike-slip fault as well as the stress changes along the fault plane directions (1 and 2 in Figure 1). The stress changes in the direction perpendicular to the fault plane (fault-normal stress) are shown in Figure 2a (middle). It emerges from these calculations that the three diagonal terms of coseismic stress changes ($\Delta\sigma_{ii}$) are substantially different in amplitude. In particular, the largest amplitudes are found for the component oriented along the slip direction and that perpendicular to the fault plane, respectively. Similar results have been obtained for a normal fault. The stress change is maximum in the direction of slip; this means $\Delta\sigma_{11}$ for a strike slip fault. This result is also evident at depth, as shown in the vertical cross sections in Figure 3. This implies that the condition $\Delta\sigma_{11} = \Delta\sigma_{22} = \Delta\sigma_{33}$, which leads to (4), is not satisfied in the volume surrounding the fault; moreover, the spatial variations of these stress components are quite different. This observation further supports the conclusion that (3) must be justified by different considerations, rather than assuming $\Delta\sigma_{11} = \Delta\sigma_{22} = \Delta\sigma_{33}$.

[34] In Figure 4 we show the Coulomb stress changes calculated both by (4) (the constant effective friction model) and by (1) and (2) (the isotropic model, see *Beeler et al.* [2000]). The two maps on the top of Figure 4 represent the Coulomb stress changes computed using the same values of friction and Skempton parameters (0.75 and 0.47, respectively). In Figure 5 we show a similar comparison for a normal fault in vertical cross section. It emerges from these
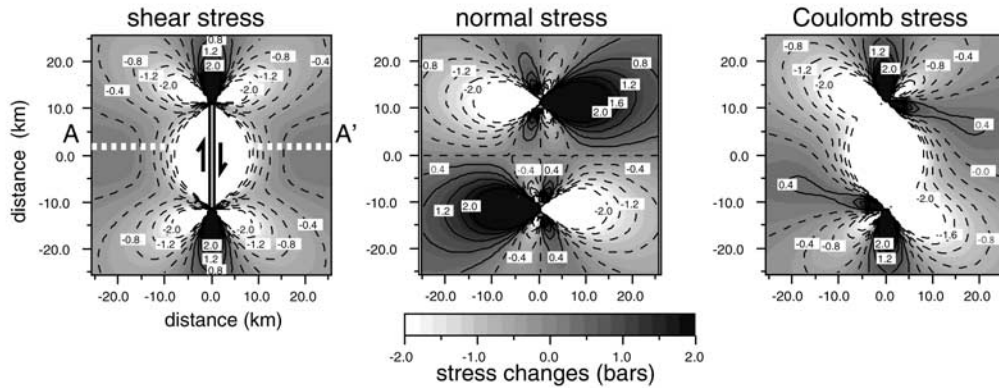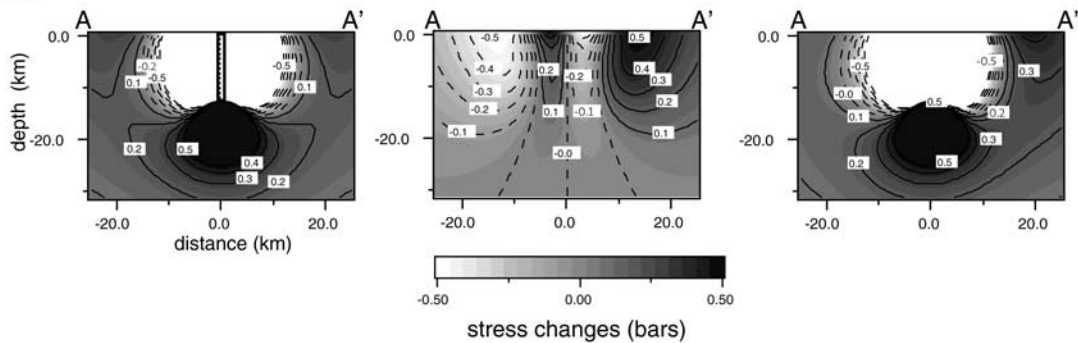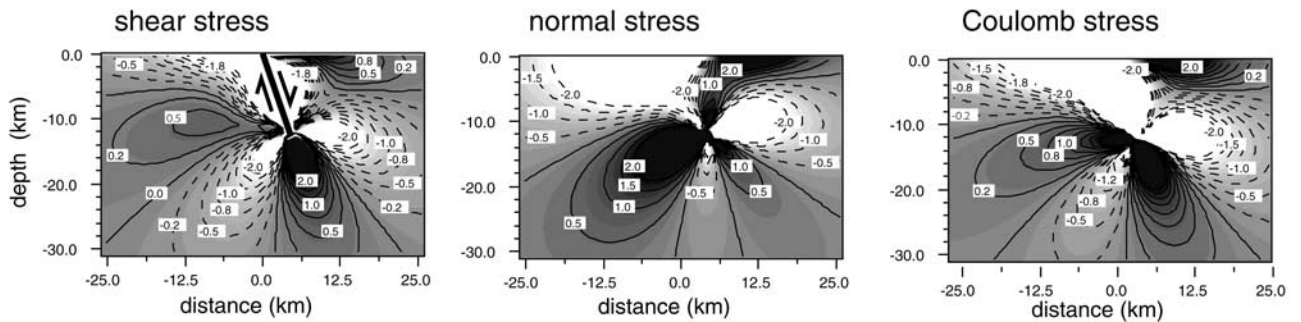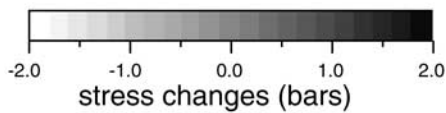
Figure 2. Shear, normal, and Coulomb stress changes caused by (a) a vertical strike-slip fault and (b) a 70° dipping normal fault calculated using the constant effective friction model of equation (4). The amount of slip on the rupturing fault is 50 cm. Coulomb stress changes have been computed on secondary fault planes having the same geometry and mechanisms as the causative faults. For all these calculations, $\mu' = 0.4$, which corresponds to $\mu = 0.75$ and $B = 0.47$. The vertical cross section for the normal fault case shown in Figure 2b is taken in the middle of the causative fault.

Volumetric Stress Changes
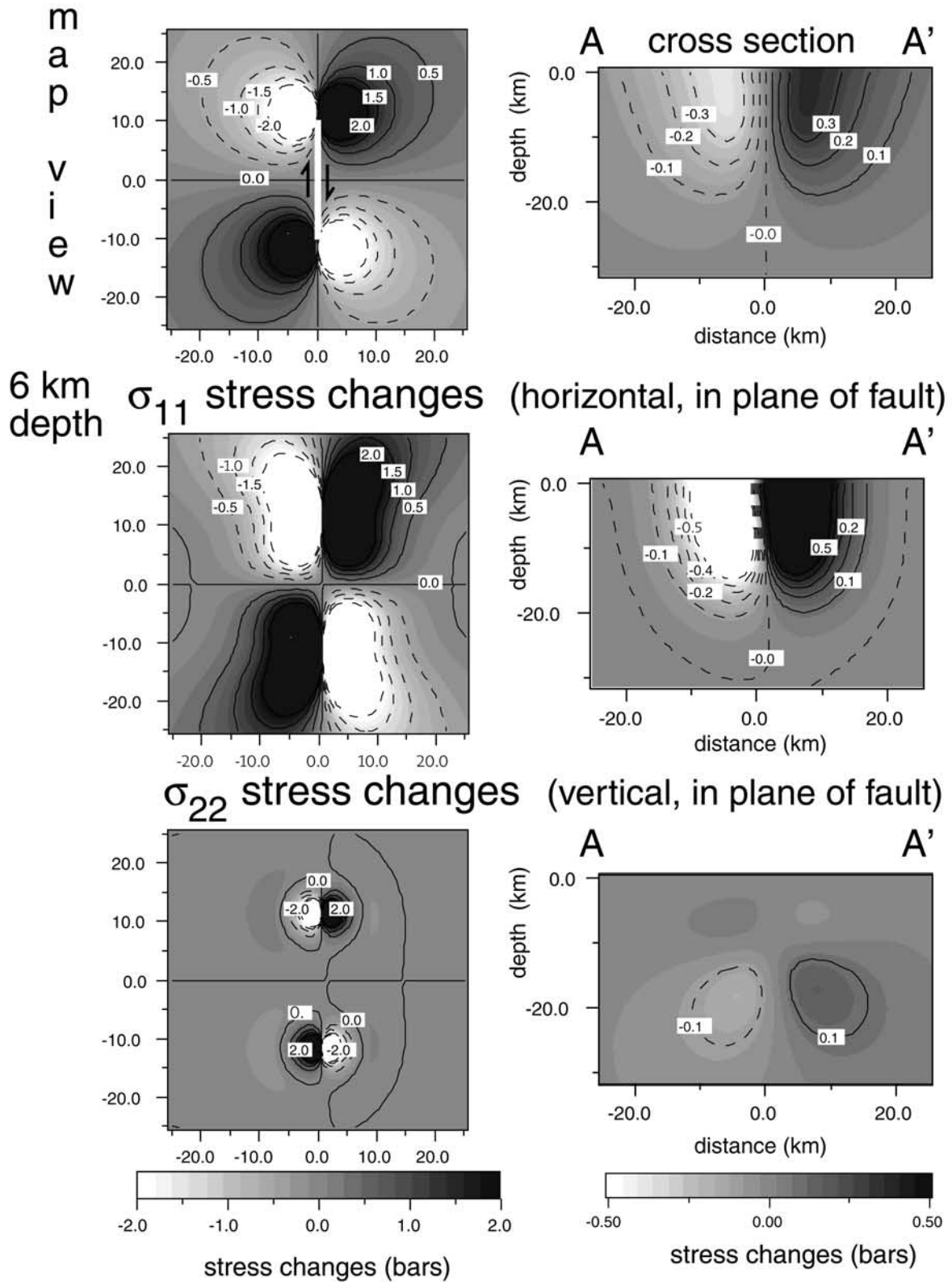
Figure 3. Map view and vertical cross section of mean stress changes ($\Delta\sigma_{kk}/3$) and induced stress perturbations for the two isotropic components oriented along the fault directions (1 and 2 of Figure 1) caused by a vertical strike-slip fault as shown in Figure 2a.
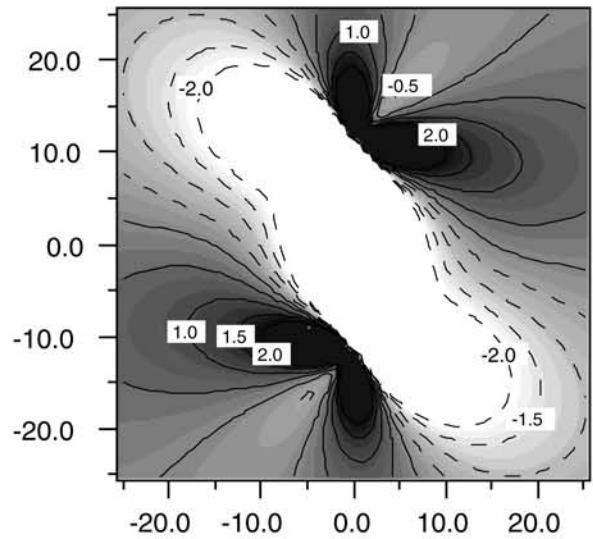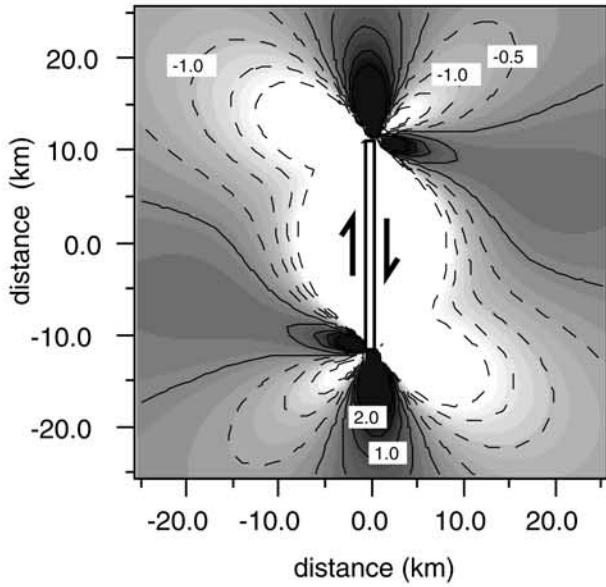
constant apparent friction
$$\Delta CFF = \Delta\tau + \mu'\Delta\sigma_n$$

isotropic model
$$\Delta CFF = \Delta\tau + \mu(\Delta\sigma_n + B\Delta\sigma_{kk}/3)$$

$$\mu' = 0.4; \quad \mu = 0.75; \quad B = 0.47$$
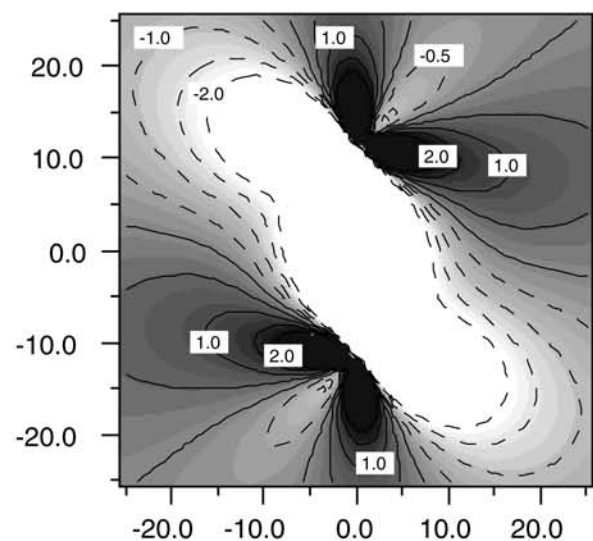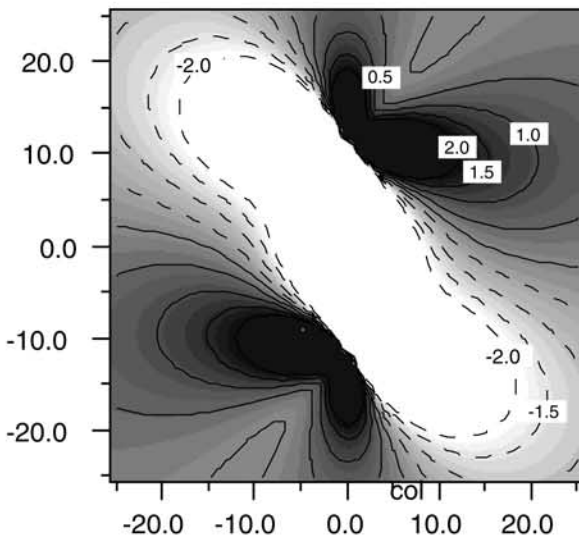
isotropic model
$$\Delta CFF = \Delta\tau + \mu(\Delta\sigma_n + B\Delta\sigma_{kk}/3)$$
$$\mu = 0.75 \; ; \; B = 1.0$$

isotropic model
$$\Delta CFF = \Delta\tau + \mu(\Delta\sigma_n + B\Delta\sigma_{kk}/3)$$
$$\mu = 0.75 \; ; \; B = 0.2$$

map view
depth = 6 km
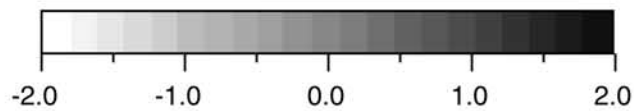
Coulomb stress changes

Figure 4. Coulomb stress changes at 6 km depth caused by a vertical strike-slip fault computed with the constant apparent friction model (equation (4)) and the isotropic friction model (equations (1) and (2)). For this latter model we show the calculations using different values of the friction and Skempton coefficients.

Figure 5. Same calculations as Figure 4 shown in a vertical cross section (as in Figure 2b) for a 70° dipping normal fault.

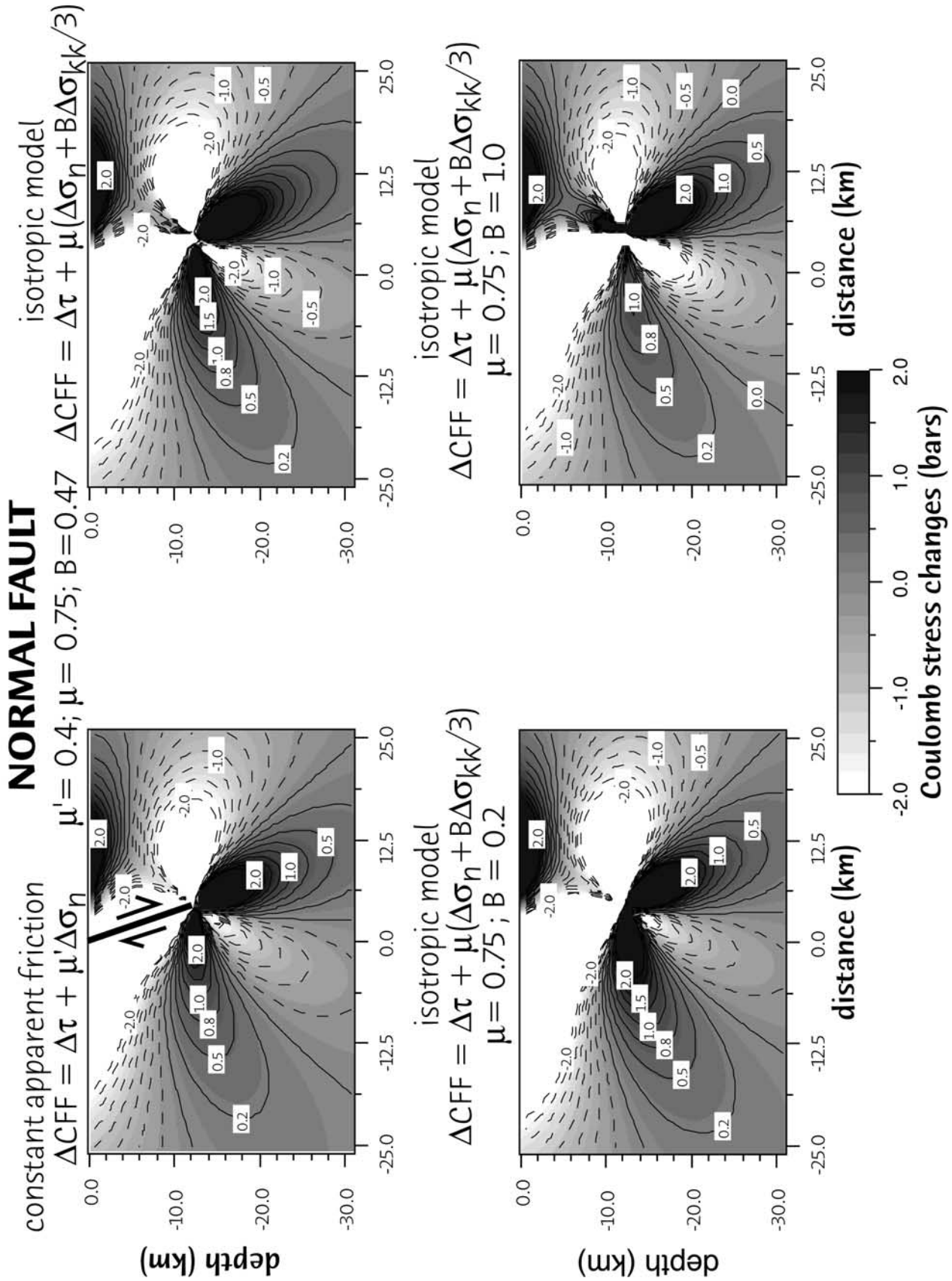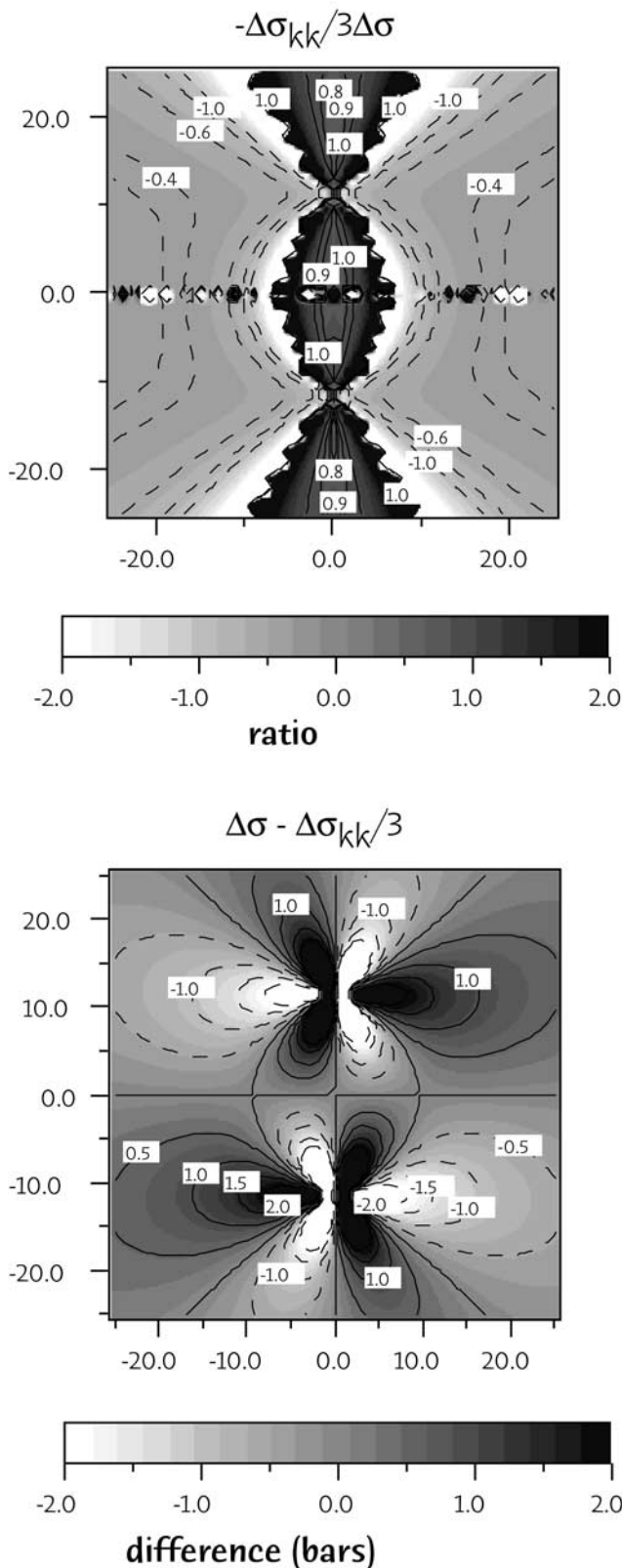**Figure 6.** (a) Spatial pattern of the ratio between mean stress perturbations (changed in sign: $-\Delta\sigma_{kk}/3$) and fault-normal stress changes ($\Delta\sigma = \Delta\sigma_{33}$) for a vertical strike slip fault. (b) Spatial pattern of the difference between normal and mean stress changes ($\Delta\sigma_{kk}/3$). Worthy of note is the amplitude of such a difference.

calculations that the equation adopted for computing Coulomb stress affects the resulting spatial patterns. Such a result has been already discussed by *Beeler et al.* [2000], who also quantified the amount of such variations. They concluded that these two pore pressure models yield considerable differences in the calculated Coulomb stress changes for reverse, normal, and strike-slip faults. They also suggest that the use of the constant effective friction model (equation (4)) could lead to errors in estimating coseismic stress changes. The calculated Coulomb stress changes also depend on the assumed value of the Skempton parameter B [see also *Beeler et al.*, 2000]. In Figures 4 and 5 we show the results of calculations using three different values of B between 0.2 and 1. As expected, increasing B increases the Coulomb stress changes in the off-fault lobes. This emphasizes the role of pore fluid pressure in earthquake failure [see, e.g., *Segall and Rice*, 1995] but also brings up the question of which is the most appropriate way to represent coseismic pore pressure changes. The differences among the Coulomb stress changes shown in Figures 4 and 5 can be as large as several bars.

[35] To summarize, we have calculated the ratio between the mean stress (changed in sign: $-\Delta\sigma_{kk}/3$) and the fault-normal stress changes $\Delta\sigma(= \Delta\sigma_{33})$(see Figure 6a). Figure 6a shows that there is a region along the fault strike direction where this ratio is highly variable. Outside this region, on the two opposite sides of the fault, this ratio is negative and smaller than unity: This means that the mean stress and the fault-normal stress changes have the same sign but the latter is larger than the former. On the contrary, in the area where the ratio is positive they have opposite sign. A unitary value for this ratio would imply that $\Delta p' = -B'\Delta\sigma$. The strike direction and that perpendicular to it are nodal for both these stress changes; thus, in these zones the amplitudes of both mean stress and fault-normal stress changes are very small (see Figures 2a and 3). In the off-fault lobes, where both mean and fault-normal stress change amplitudes are relevant, this ratio is negative and smaller than unity. This is quite evident in Figure 6b, where we plot the difference between normal and mean stress changes. These two terms differ mostly at the ends of the slipped zone. The implication of these calculations is that the effective friction coefficient is not constant in the volume surrounding the causative fault. This is expected, since from its definition it is a function of ratios of all the fault-normal stress changes to one another in the medium.

[36] The considerations discussed above point out that in a poroelastic isotropic medium the relation used to compute pore pressure changes affects the calculation of Coulomb stress changes. Effective normal stress depends on both mean stress and fault-normal stress changes, and the proportionality factors do not vanish, except in very special situations that might not be realistic for actual fault zones. Moreover, the amplitudes of these stress changes show different spatial patterns, depending on the faulting mechanism [see also *Beeler et al.*, 2000]. Therefore, in order to choose the appropriate equation to compute Coulomb stress it is necessary to consider more complex situations and different properties for the fault zone materials.

6. Effects of Anisotropy Within the Fault Zone

[37] The results discussed above have been obtained under the assumption that the fault zone materials are isotropic, i.e., that they are permeated by an isotropic distribution of cracks that are saturated by fluids. However, anisotropy within the fault zone caused by aligned fractures may lead to different conclusions concerning the proportionality between pore pressure and fault-normal stress changes. Here we examine the effect of an anisotropic distribution of cracks within the fault zone, and we derive an alternative formulation for the pore pressure changes for undrained deformation. Because we are interested here in the undrained response of the medium, we do not discuss the anisotropy of permeability of the fault zone materials.

[38] In the general case, possibly anisotropic, equation (2), which introduces the Skempton coefficient, must be generalized to the statement that a pore pressure change

$$\Delta p = -B_{ij}\frac{\Delta\sigma_{ij}}{3} \qquad (20)$$

is induced by application of stress changes $\Delta\sigma_{ij}$ under undrained conditions. The set of coefficients B_{ij} constitute what we propose to call a Skempton tensor. They reduce, of course, to $B_{ij} = B\delta_{ij}$ in the isotropic case. If we regard P as a function of the set of stresses $[\sigma]$ and of the fluid mass m, per unit volume of reference state, contained in the porous material, that is, $p = p([\sigma], m)$, then B_{ij} satisfy

$$B_{ij} = 3\{\partial p([\sigma, m])/\partial\sigma_{ij}\}. \qquad (21)$$

[39] We show in Appendix A that an alternative, and instructive, interpretation can be obtained for that partial derivative once we recognize [*Rice and Cleary*, 1976] that $\sigma_{ij}d\varepsilon_{ij} + pd(m/\rho)$ must be a perfect differential, where ρ is the density of the pore fluid (conceptually in a reservoir of pure fluid at local equilibrium with the porous medium). Here it may be noted that m/ρ is the fluid volume fraction (fluid volume per unit of reference state volume of the porous material) in the case considered, when all pore space is connected and fluid-infiltrated. The mass of fluid per unit reference state volume is m and ρ ●is the density of pore fluid at pressure p, and we assume $\rho = \rho(p)$. The differential form sums the work of stresses in moving the boundaries of an element of the porous material and the work of pore pressure in enlarging the boundaries of the pore space. Together the terms constitute the change dU in the strain energy U of the solid phase, which must be a function of state. As developed in Appendix A, this is equivalent to the familiar notion from the thermodynamics of mixtures that $\sigma_{ij}d\varepsilon_{ij} + \hat{\mu}dm$ $\sigma_{ij}d\varepsilon_{ij} + \hat{\mu}dm$ is a perfect differential, where $\hat{\mu}$ is the chemical potential of the pore fluid.

[40] By either route, the existence of the perfect differentials implies a Maxwell reciprocal relationship, which is shown in Appendix A to give the alternative interpretation of B_{ij} as

$$B_{ij} = 3\rho\{\partial\varepsilon_{ij}([\sigma, m])/\partial m\}. \qquad (22)$$

The derivative corresponds to the change as fluid mass is pumped into the porous material under conditions for which all of the stresses σ_{kl} are held fixed.

[41] Thus, for example, in the isotropic case $B/(3\rho)$ is the increase of each extensional strain per unit of increase dm of fluid mass pumped into the material, under conditions for which the total stresses are held constant. Equivalently, $B/3$ is the increase of each extensional strain per unit increase dm/ρ of fluid volume pumped in under constant stresses.

[42] Let suppose that within the fault zone there is a highly anisotropic distribution of cracks or flattened pores, lying so that their long directions are approximately parallel to the fault plane. We isolate a sample of material of the fault and subject it to its in situ stress state σ'_{kl}. Then, holding those stresses constant, we pump an increment dm' of fluid mass into the porous material. In that case, because of the assumed orientations of the flattened pores we would expect the fault-parallel strain increments $d\varepsilon'_{11}$ and $d\varepsilon'_{22}$ to be much smaller than the fault-normal component $d\varepsilon'_{33}$ because it is the latter which would be primarily influenced by fluid injection into the fault parallel-crack and pore space. That means B'_{33} is much larger than the other components of B'_{ij}, and therefore that

$$dp' = -B'_{ij}\frac{d\sigma'_{ij}}{3} \approx -B'_{33}\frac{d\sigma'_{33}}{3} = -B'_{33}\frac{d\sigma_{33}}{3}. \qquad (23)$$

Hence, for that type of anisotropy of pore space, which may be appropriate for a fault zone, it is correct to use the simplified concept that induced pore pressure under undrained conditions is determined solely by the change in fault-normal stress. In other words, if the anisotropy of the fault zone material is so extreme that when extracted from the fault and held at constant stress while fluid is pumped into it, it expands only in the 3 direction, then p' would be determined solely by $\sigma'_{33} = \sigma_{33}$, and then the μ' concept would apply exactly with $\hat{B}; = B'_{33}/3$ in equation (3).

[43] It might be interesting to know how much anisotropy is needed to justify the effective friction concept in the way just discussed. Recent papers on fault zone trapped waves [*Leary et al.*, 1987; *Zhao and Mizuno*, 1999] have shown very good quality data, but unfortunately, there is still no answer to this question. *Zhao and Mizuno* [1999] found a crack density distribution for the 1995 Kobe (Japan) earthquake that is smaller (0.2) than that expected for a fracture zone (0.6–0.75). It is important to point out that the presence of anisotropy within the fault zone may justify variations of shear wave velocity of 50% and larger. Future observations are needed to shed light on this problem; they will be helpful to reconstruct the inner structure and mechanical properties of fault zone materials.

7. Short Time Pore Pressure Equilibrium Between Fault Zone and Adjoining Rock Mass

[44] We have focused thus far on the postseismic period, in which the fault zone behaves as if it is undrained. However, if the fault zone is moderately thin and has some permeability, then it is reasonable to expect that on what is also a relatively short time-scale, the fault zone will act as if it were locally drained and reach pressure equilibrium with its surroundings, so that $\Delta p'$ evolves toward Δp. Δp itself will be time-dependent because of the pore fluid fluxes set up by the gradients in the coseismically induced pore pressure field, but unless the fault zone is very thick and/or is very impermeable compared to its surroundings, that variation of P in the adjoining rock will have a much longer timescale than for local drained response of the fault. In such cases it is reasonable to expect that $\Delta p'$ will have relaxed to Δp well before Δp itself has relaxed much from its undrained value just after the earthquake stress change. So, on such short but not extremely short timescale in which the fault acts as drained, but its surroundings remain undrained, we get $\Delta p' \approx \Delta p$ and thus $\Delta p'$ is proportional to the mean stress change outside the fault zone, $\Delta p' \approx -\Delta\sigma_{kk}/3$.

[45] In order to model this behavior in a simple way, we consider a fault zone of thickness h (see Figure 1) having a uniform permeability k', fluid viscosity η', and storage modulus N'. The surrounding crust is modeled as a pair of semi-infinite domains with corresponding parameters N, k, η. The storage modulus is just the inverse of the storage coefficient (called S by *Wang* [2000]), in response to pore pressure changes, for one-dimensional straining under constant stress in the straining direction. See Appendix B for its precise definition and expression in terms of moduli already introduced. As shown in Figure 1, the axis 3 is perpendicular to the fault. The diffusivity inside the fault zone (c') and in the surrounding medium (c) can be respectively defined as

$$c' = k'N'/\eta \qquad c = kN/\eta,$$

which depend on the viscosity, the permeability, and the storage modulus (the increase of fluid mass content when the pressure varies under one-dimensional strain conditions) of the fault and of the surrounding crust.

[46] By solving the one-dimensional consolidation problem for a layer of one porous medium within an effectively infinite outer one, we model the evolution of the pore pressure within the fault zone toward its longer time limit Δp. The pore pressure inside the

fault zone ($\Delta p'$) is a function of time and position in the fault zone, but for simplicity, we solve the problem at the center of the fault zone (Appendix B). However, in the following, we will derive an analytical expression for the pore pressure at any point inside the fault zone. Our analysis of short-time undrained response shows that at time $t = 0^+$ the fault zone has the pore pressure change $\Delta p'$ (given by equation (13)), whereas the surrounding crust has the change $\Delta p = -B\Delta\sigma_{kk}/3$. We determine the subsequent temporal evolution by finding the difference between the pore pressure inside and outside the fault zone, normalized by its value just after the time of the main shock ($t = 0^+$):

$$\Delta\tilde{P} = \frac{\Delta p'(t) - \Delta p}{\Delta p'(0^+) - \Delta p}. \tag{24}$$

[47]   Here the notation $\Delta p'(t)$ denotes $\Delta p'(z, t)|_{z=0}$,i.e.,the pore pressure change at the center of the fault zone. In AppendixB we solve simple diffusion equations using the Laplace transform and its Bromwich inversion to find an expression for the variable defined in (24)that depends on the parameter r, which is the ratio of diffusivities and storage moduli inside and outside the fault zone:

$$r = \left(\frac{k'/\eta'}{k/\eta}\right)\frac{N}{N'} = \frac{c'}{c}\left(\frac{N}{N'}\right)^2.$$

[48]   Once the solution is found (equation(B2) in Appendix B), we estimate what parameters control the timescale over which the fault zone reaches pressure equilibrium with its surroundings. In Appendix B we show that the time at which the pore pressure at the center of the fault has evolved approximately half way toward its longer time limit of Δp is given by

$$t_d = \frac{h^2}{8c'} + \frac{h^2}{8c}\left(\frac{N}{N'}\right)^2 = \frac{h^2}{8c'}(1 + r). \tag{25}$$

[49]   This time constant is the sum of a characteristic drainage time for the fault core plus a characteristic time for the crust. Two limit cases exist: when$r$=0, the crust is much more permeable than the fault zone, and more interesting ly, when $r\rightarrow\infty$, the fault zone is much more permeable than the surrounding crust. In the former case the time constant is simply t_d=$h^2/8c'$, while the latter condition yields

$$t_d = \frac{h^2}{8c}\left(\frac{N}{N'}\right)^2.$$

[50]   In Figure 7 we show the temporal evolution of the normalized pore pressure alteration (defined in (24)) for short and long timescales and for different values of the parameter r. Figure 7 shows that the solution for $r\geq4$ is almost identical to that obtained for $r = \infty$. The pore pressure alteration at the fault center is halfway toward its longer time limit after a time which varies from 0.75 t_d when $r = 0$, to 1.20 t_d when $r = \infty$. This property is what motivated our definition of t_d. We may also note that for all cases except $r = 0$, there is a slow evolution at long times, and thus the process is not readily characterized solely by t_d. Indeed, the asymptotic evaluation of the solution (B2) for large t shows that

$$\frac{\Delta p'(t) - \Delta p}{\Delta p'(0^+) - \Delta p} \rightarrow \sqrt{\frac{2rt_d}{\pi(1+r)t}} = \frac{h}{2\sqrt{\pi ct}}\frac{N}{N'},$$

A) pore pressure evolution short timescale
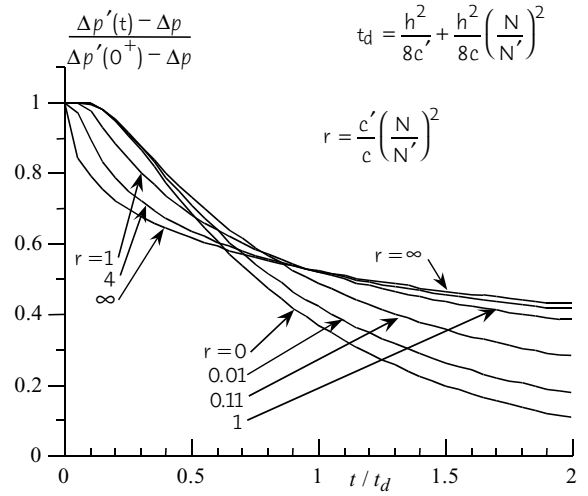
B) pore pressure evolution long timescale
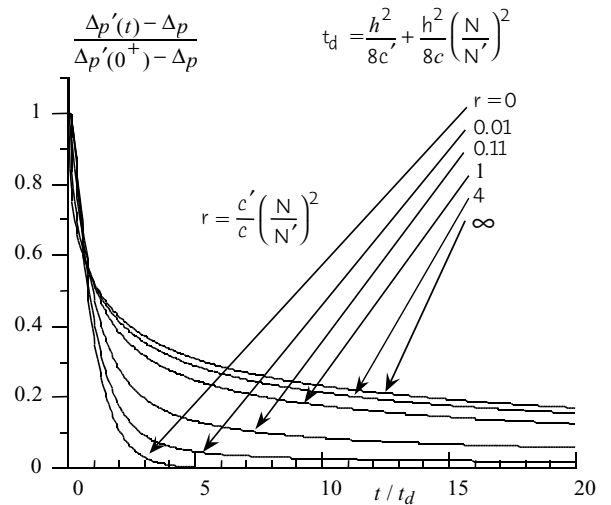
Figure 7. Temporal evolution of normalized pore pressure alteration at a (a) short and (b) long timescales for different values of the parameter r(see text for its definition). The time variable is normalized using the characteristic time for pore pressure equilibrium, while the pore pressure alteration is normalized at its initial value at the instant of application of the induced stress.

representing a slow temporal decay as $t^{-1/2}$. This slow asymptotic decay rate is independent of the permeability within the fault zone, although the time at which that asymptotic expression becomes accurate does depend on fault permeability, since it enters in the ratio r. Infact, that asymptotic form, which is instructively written as

$$\Delta p'(t) - \Delta p \rightarrow \frac{N}{2\sqrt{\pi ct}}\frac{\Delta p'(0^+) - \Delta p}{N'}h,$$

is valid in the generalized form

$$\Delta p'(t) - \Delta p \rightarrow \frac{N}{2\sqrt{\pi ct}}\int_{-h/2}^{+h/2}\frac{\Delta p'(z, 0^+) - \Delta p}{N'(z)}dz \tag{26}$$

when we do not assume that the poroelastic material properties are uniform within the fault zone. Rather, in (26) we assume that all material properties vary with position z within the fault zone, such as $N' = N'(z)$ but are uniform outside it (at $|z| > h/2$). Here $\Delta p = -B\Delta\sigma_{kk}/3$ as before in the adjoining crust, and (26) applies on a sufficiently long timescale that local pore pressure equilibrium is achieved within the fault zone, with $\Delta p'(t)$ denoting that value. Also, $\Delta p'(z, 0^+)$ is the pore pressure change that would have been induced at position z (which coincides with the axis 3 in Figure 1) within the fault zone in undrained response to the stress change. It is given by our earlier expression for $\Delta p'$ as a linear combination of $\Delta\sigma_{kk}/3$ and $\Delta\sigma_{33}$ but now written as

$$\Delta p'(z, 0^+) = -B'(z)\frac{K_u'(z)}{M_u'(z)}\left[\frac{G'(z)}{G}\frac{M_u}{K_u}\frac{\Delta\sigma_{kk}}{3} + \frac{G - G'(z)}{G}\Delta\sigma_{33}\right]$$

This allows, for example, for a fault core and bordering zone with damage degrading gradually toward that appropriate for the surrounding crust.

[51] It is interesting to provide a tentative evaluation of the characteristic time values for local pressure equilibrium. It emerges from (25) that the characteristic time will be dominated by the smallest value of diffusivity, c or c', which effectively means the smallest permeability, since it is reasonable to assume that the storage modulus and the fluid viscosity do not significantly change between the fault zone and the surrounding crust. In Table 1 we list the values of $t_d = h^2/8c_{min}$, understanding for c_{min} the smaller diffusivity value. We assume a fluid viscosity of 2×10^{-4} Pa s and a storage modulus of 100 GPa. We have calculated the characteristic times for two values of permeability: 10^{-18} m^2 and 10^{-21} m^2, respectively, and for fault thickness in the interval 1 mm $\leq h \leq$ 1 km. As expected, the resulting values of the characteristic time for local pressure equilibrium change from seconds to years. This suggests that it is really difficult to exclude a priori the contribution of time-dependent pore pressure equilibrium in the analysis of stress redistribution. Moreover, a complex fault network will inevitably have segments at different stages of their relaxation from undrained conditions to local pressure equilibrium with the nearby materials.

8. Discussion and Concluding Remarks

[52] Postseismic stress redistribution is a time-dependent process, and at short or intermediate timescales (from minutes to few years after a seismic event), fluid flow can be one of the most important factors in contributing to this temporal variation of the stress perturbation [*Nur and Booker*, 1972; *Hudnut et al.*, 1989; *Noir et al.*, 1997]. In order to properly include a pore pressure model in Coulomb analysis through equation (1) it is necessary to choose the timescale during which the stress changes are modeled as well as to make a few assumptions on the material properties of the medium. In this study we have investigated two different timescales. We have first focused our attention on the short-term postseismic period, in which both the fault zone and the adjoining lithosphere respond under undrained conditions. Thus we neglect the alteration of pore pressure caused by fluid flow. In this first configuration we discuss the pore pressure changes both in an isotropic poroelastic medium and in an anisotropic fault zone.

[53] That first condition allows a comparison with most of the Coulomb stress studies. We have derived an analytical expression that relates pore pressure changes for undrained deformation within the fault zone to mean and fault-normal stress changes for an isotropic poroelastic medium. Both these terms contribute to the variations of pore pressure caused by the stress redistribution process. Their relative weight in the derived equation depends on the contrast between the elastic parameters inside the fault zone

Table 1. Characteristic Times for Local Pressure Equilibrium

Fault Thickness h, m	Permeability	
	$k = 10^{-18}$ m^2	$k = 10^{-21}$ m^2
0.001	2.5×10^{-4} s	0.25 s
0.01	2.5×10^{-2} s	25.0 s
0.1	2.5 s	42 min
1.	4.2 min	2.9 days
10	6.9 hours	9.7 months
100	29 days	80 years
1000	8.0 years	80 centuries

and those of its surroundings. We have shown that if the rigidity inside the fault zone is much smaller than that in the surrounding crust, which should correspond to a large reduction of S wave velocity within the fault zone, the pore pressure is primarily controlled by the fault-normal stress changes and the definition of the effective friction coefficient given in literature is tenable. However, we emphasize that if the fault zone is an isotropic poroelastic medium permeated by fluids, the fault-normal stress changes are the most important factor controlling the pore pressure changes only when the reduction in S wave velocity is >50%. A limiting case, for which only the mean stress (i.e., the first invariant) controls the pore pressure, is found for faults whose rigidity is equal to that of the surrounding crust. However, such a condition appears inconsistent with observations of fault zone structure resulting from seismic tomography and fault zone trapped-wave studies. These studies consistently show that body wave velocities within the fault zone are different from those in the surrounding crust. In particular, fault zone trapped-wave studies indicate that shear wave velocities in fault zones are as much as 50% smaller than in their surroundings. If the fault zone materials do not behave as in these extreme conditions, both the mean stress and the fault-normal stress changes contribute together to the pore pressure changes for undrained deformation during such a short timescale.

[54] Calculations of Coulomb stress changes caused by shear dislocations in an elastic isotropic half-space show that the choice of the pore pressure model influences the results significantly. In particular, we show that the use of a constant effective friction model (equations (3) and (4)) as opposed to an isotropic and homogeneous pore pressure model (equations (1) and (2)) implies very different Coulomb stress changes [see also *Beeler et al.*, 2000]. These stress changes also depends on the assumed values of friction and Skempton parameters.

[55] We also briefly investigated the effect of anisotropy in the cracked region forming the fault core. In this case, the Skempton parameter becomes a tensor. However, it is plausible to assume that the strain component normal to the fault is much larger than those in the fault-parallel directions. In that case, the pore pressure should be solely dependent on the fault-normal stress, and the definition of the effective friction coefficient should be correct. Thus we can conclude that at very short postseismic time periods in which the fault zone obeys undrained conditions, the constant effective friction model could be an acceptable approximation only under quite extreme conditions, such as if the fault zone rigidity is <50% that of its surroundings or if the fault zone is strongly anisotropic. This latter configuration would be approached if porosity is dominated by an oriented distribution of cracks or flattened pores aligned with their long directions subparallel to the fault plane.

[56] We have also discussed an intermediate timescale, which will exist only for a sufficiently permeable fault that is locally drained and reaches pressure equilibrium with its surroundings. In this time period the adjoining lithosphere is still responding as if it were effectively undrained. In this case, we assume that the fault zone is moderately thin and has some permeability. During this

relatively short timescale, $\Delta p'$ evolves toward Δp, the former being time-dependent due to the pore fluid fluxes generated by gradients in the coseismically induced pore pressure field. This variation of P in the adjoining rock will be slower than the local drained response of the fault. Therefore, on such a short but not extremely short timescale, during which the fault acts as drained, but its surroundings do not, we get $\Delta p' \approx \Delta p$, and thus $\Delta p'$ is proportional to the mean stress changes. The characteristic time of this local pressure equilibrium depends on the permeability and the fault thickness.

[57] The transition from short-term undrained to drained response in the adjoining lithosphere occurs in general on a yet longer timescale. This should always occur as time increases, except when the fault zone is hydrologically isolated from its surroundings. In these circumstances, the stress changes $\Delta\sigma_{ij}$ approach the values that would be calculated from elastic dislocation theory using drained, rather than undrained, elastic moduli. The drained response is elastically less stiff than the undrained response: $K < K_u$, $v < v_u$, $G = G_u$. In general, we might expect that this transition from undrained to drained response modestly reduces the stress changes. For a mode II shear crack, in a plane strain condition, the reduction scales as $(1 - v_u)/(1 - v)$. For Westerly granite this value is close to 0.9; thus the stress reduction at longer time periods seems almost negligible. However, a complete recognition of this behavior during such longer timescale is beyond the aims of the present study.

[58] The time dependence is included in the Coulomb failure function not only through the pore pressure changes Δp (equation (1)). In fact, poroelastic theory shows that there is a time dependence of all the stress components σ_{ij} (we have considered here only timescales for which those σ_{ij} are effectively constant outside the fault zone). *Nur and Booker* [1972] pointed out that the time dependence of pore pressure changes can interact with seismicity explaining aftershocks, and *Rice* [1980] evaluated the resulting time-dependent postseismic shear stress history on a fault surface. Further observations are needed to image the inner structure of fault zones and therefore to verify the most appropriate pore pressure model. In absence of constraining evidence we cannot exclude any model for including pore pressure in Coulomb failure. However, at least in a homogeneous and isotropic poroelastic medium, the influence on pore pressure of the mean stress is well established.

Appendix A. Induced Pore Pressure for Undrained Stressing of an Anisotropic Medium and Interpretation of a Skempton Tensor

[59] An increment of work (per unit volume of the reference state) done on a poroelastic material, precisely on its solid phase, is given by $\sigma_{ij}d\varepsilon_{ij} + pd(m/\rho)$ [e.g., *Rice and Cleary*, 1976], where m/ρ is the fluid volume fraction defined as in the text. We recall that m is the mass of fluid per unit reference state volume of porous material and ρ ●is the density of pure fluid at pressure p, and we assume $\rho = \rho(p)$. This increment of work must be a perfect differential of a function of state (i.e., of the strain energy U of the solid phase, or of its Helmholtz free energy, at the constant temperature conditions considered), and so

$$\sigma_{ij}d\varepsilon_{ij} + pd(m/\rho) = dU. \tag{A1}$$

[60] Introducing the "chemical potential" $\hat{\mu} = \hat{\mu}(p)$ by

$$\hat{\mu} = \hat{\mu}(p) = \int_{p_0}^{p} \frac{1}{\rho(\hat{p})} d\hat{p}, \tag{A2}$$

where p_0 is an unessential reference pressure, we may use the property that $d\hat{\mu} = dp/\rho$ to obtain

$$pd\left(\frac{m}{\rho}\right) = d\left(\frac{pm}{\rho}\right) - \left(\frac{m}{\rho}\right)dp \tag{A3}$$

$$= d\left(\frac{pm}{\rho}\right) - md(\hat{\mu}) = d\left(\frac{pm}{\rho} - \hat{\mu}m\right) + \hat{\mu}dm.$$

Thus (A1) can be transformed to another perfect differential which is well known in the thermodynamics of mixtures, namely,

$$\sigma_{ij}d\varepsilon_{ij} + \hat{\mu}dm = d\left(U + \hat{\mu}m - p\frac{m}{\rho}\right). \tag{A4}$$

[61] While it is unessential for what follows, the expression of (A2) for $\hat{\mu}$ may be seen to be consistent with interpreting $\hat{\mu}dm$ as the total reversible work of extracting an element of mass dm from a reservoir of fluid at a reference pressure and fluid density (p_0, $\rho_0 = \rho(p_0)$), and inserting it (say, through a porous screen) into a porous medium at a place where the pore pressure and fluid density are (p, ρ). We assume that temperature is the same in the reservoir as in the place of insertion and calculate the work in three steps, as follows: (1) work of withdrawal from reservoir, $-p_0dm/\rho_0$ (note that dm/ρ_0 is the volume withdrawn from the reservoir), (2) work of changing density from ρ_0 to ρ, which is $-dm\int_{\rho_0}^{\rho}pd(1/\rho)$. (3) Work of inserting the fluid at the place where pressure is p, which is pdm/ρ (dm/ρ is the volume inserted). The sum is $\hat{\mu}dm$, so that

$$\hat{\mu}dm = -p_o\frac{dm}{\rho_o} - dm\int_{\rho_o}^{\rho}pd(1/\rho) + p\frac{dm}{\rho} = dm\int_{p_o}^{p}(1/\rho)dp, \tag{A5}$$

which is consistent with the expression for $\hat{\mu}$ in (A2).

[62] By a final rearrangement, we obtain

$$-\varepsilon_{ij}\,d\sigma_{ij} + \hat{\mu}dm = dV \tag{A6}$$

as a perfect differential, where $V = U + \hat{\mu}m - p(m/\rho) - \sigma_{ij}\varepsilon_{ij}$. Regarding V as a function of the set of stresses $[\sigma]$ and fluid mass m, $V = V([\sigma], m)$, it therefore follows that

$$\hat{\mu} = \frac{\partial V([\sigma], m)}{\partial m}; \varepsilon_{ij} = -\frac{\partial V([\sigma], m)}{\partial \sigma_{ij}}. \tag{A7}$$

Recognizing that $\partial^2 V[\sigma], m)/\partial m\delta\sigma_{ij}$ must be independent of the order of differentiation, the Maxwell reciprocal relation

$$\frac{\partial\hat{\mu}([\sigma], m)}{\partial\sigma_{ij}} = -\frac{\partial\varepsilon_{ij}([\sigma], m)}{\partial m} \tag{A8}$$

must be valid. Its left side can be rewritten as

$$\frac{\partial\hat{\mu}([\sigma], m)}{\partial\sigma_{ij}} = \left[\frac{\partial\hat{\mu}(p)}{\partial p}\right]\frac{\partial p([\sigma], m)}{\partial\sigma_{ij}} = \frac{1}{\rho}\frac{\partial p([\sigma], m)}{\partial\sigma_{ij}}, \tag{A9}$$

and so the Maxwell relation is equivalent to

$$\frac{\partial p([\sigma], m)}{\partial\sigma_{ij}} = -\rho(p)\frac{\partial\varepsilon_{ij}([\sigma], m)}{\partial m}. \tag{A10}$$

[63] We recognize that $\partial p([\sigma], m)/\partial \sigma_{ij}$ as being a generalization of the Skempton coefficient B, valid for the anisotropic case as well, and make the definition

$$\frac{B_{ij}}{3} = \frac{\partial p([\sigma], m)}{\partial \sigma_{ij}} \qquad (A11)$$

to define a Skempton tensor, with property that $\Delta p = -B \Delta\sigma_{ij}/3$ under undrained conditions. (Of course, in the isotropic case, $B_{ij} = B\delta_{ij}$.) The Maxwell relation then gives us an interpretation of, and alternative way of understanding, the Skempton tensor as

$$B_{ij} = 3\rho \frac{\partial \varepsilon_{ij}([\sigma], m)}{\partial m}. \qquad (A12)$$

Appendix B. Short-Term Pore Pressure Equilibrium Between Fault Zone and Surrounding Crust

[64] The fault is modeled as a zone of thickness h (see Figure 1), which has uniform permeability k', fluid viscosity η', and storage modulus N' (defined below). The surrounding crust is modeled as a pair of semi-infinite domains with corresponding parameters k, η, N. Our analysis of short-time undrained response shows that at time $t = 0^+$ the fault has the pore pressure change $\Delta p'$ (which we have calculated in (13) as $-B'$ times a linear combination of $\Delta\sigma_{33}/3$ and $\Delta\sigma_{33}$), whereas the surrounding crust has the change $\Delta p = -B\Delta\sigma_{kk}/3$.

[65] The poroelastic equations then allow us to model the evolution of the pore pressure in the fault toward its longer time limit $\Delta p = -B\Delta\sigma_{kk}/3$. Recognizing that only ε_{33} and no other strain varies with time, and noting that σ_{33} is uniform, the same inside and outside the fault, the problem is recognized as one of one-dimensional consolidation. The governing equations within the fault and the crustal domains, respectively, incorporating Darcy's law and conservation of mass of the diffusing fluid, for $t > 0$ take the forms of

$$\frac{\delta}{\delta z}\left(\frac{k'}{\eta'}\frac{\delta p(z,t)}{\delta z}\right) = \frac{1}{N'}\frac{\delta p(z,t)}{\delta t}, \quad -h/2 < z < h/2$$

$$\frac{\delta}{\delta z}\left(k\eta \frac{\delta p(z,t)}{\delta z}\right) = \frac{1}{N}\frac{\delta p(z,t)}{\delta t}, \quad z > h/2, \quad z < -h/2,$$

where z is the spatial coordinate in the 3 direction, perpendicular to the fault. These are homogeneous diffusion equations for p. The general consolidation equations instead involve a homogeneous diffusion equation for m [*Rice and Cleary*, 1976], not p, but reduce to such an equation for P in the case of one-dimensional straining, like here. The diffusivities $c' = k'N'/\eta'$ and $c = kN/\eta$. Their solution will be even in z and must satisfy, for $t > 0$,

$$p\left(\frac{h^-}{2}, t\right) = p\left(\frac{h^+}{2}, t\right)$$
$$\frac{k'}{\eta'}\left(\frac{\delta p(z,t)}{\delta z}\right)_{z=h^-/2} = \frac{k}{\eta}\left(\frac{\delta p(z,t)}{\delta z}\right)_{z=h^+/2}$$

The storage modulus N (inverse of the storage coefficient) is defined such that $dm = \rho_0 dp/N$ is the increase in fluid mass content when the pressure varies under conditions of one-dimensional strain, with σ_{33} held constant. Expressions for it can be extracted from those for c in the sources mentioned on poroelasticity [*Biot*, 1941, 1956; *Rice and Cleary*, 1976; *Kuempel*, 1991; *Wang*, 2000],

since $N = c\eta/k$. Thus, from equation (17) of *Rice and Cleary* [1976], but with their expressions in terms of Poisson ratios rewritten in terms of moduli used earlier here, we have $N = B^2 K_u^2 M/(K_u - K)M_u$.

[66] Measuring P relative to its value at time $t = 0^-$ (just before the earthquake), so that $p = \Delta p'$ in the fault zone and Δp outside in the crust at $t = 0^+$, and letting

$$\hat{p}(z,s) = \int_0^\infty p(z,s)e^{-st}dt$$

be the Laplace transform, the solution of the above equation set is

$$\hat{p}(z,s) = \frac{\delta p'(0^+)}{s} - \frac{[\Delta p'(0^+) - \Delta p]\cosh[z\sqrt{s/c'}]}{s\{\cosh[(h/2)\sqrt{s/c'}] + \sqrt{r}\sinh[(h/2)\sqrt{s/c'}]\}} \quad z|z| < h/2$$

$$\hat{p}(z,s) = \frac{\Delta p}{s} + \frac{[\Delta p'(0^+) - \Delta p]\sqrt{r}\sinh[(h/2)\sqrt{s/c'}]\exp[-(|z| - (h/2))\sqrt{s/c'}]}{s\{\cosh[(h/2)\sqrt{s/c'}] + \sqrt{r}\sinh[(h/2)\sqrt{s/c'}]\}} \quad |z| > h/2,$$

where now $\Delta p'(0^+)$ is the same as $\Delta p'$ of (13), and the parameter:

$$r = \frac{\left(\frac{\kappa'}{\eta'}\right)N}{\left(\frac{\kappa}{\eta}\right)N'} = \frac{c'}{c}\left(\frac{N}{N'}\right)^2.$$

[67] It is simplest to invert the transform solution for the pore pressure at the center of the fault zone, and we use the notation

$$\Delta p'(t) \equiv p(0, t),$$

so that

$$\Delta\hat{p}'(s) \equiv \hat{p}(0, s).$$

Then

$$\frac{\Delta\hat{p}'(s) - \Delta p/s}{\Delta p'(0^+) - \Delta p} \equiv \frac{1}{s}\left(1 - \frac{1}{\cosh[(h/2)\sqrt{s/c'}] + \sqrt{r}\sinh[(h/2)\sqrt{s/c'}]}\right).$$

The Bromwich inversion integral is then

$$\frac{\Delta p'(t) - \Delta p}{\Delta p'(0^+) - \Delta p} = \frac{1}{2\pi i}\int_{0^+-i\infty}^{0^++i\infty}\left(\frac{\Delta\hat{p}'(s) - \Delta p/s}{\Delta p'(0^+) - \Delta p}\right)e^{st}ds. \qquad (B1)$$

Since the integrand vanishes rapidly enough as $|s| \to \infty$ and has no poles (at least when $r > 0$) but has a branch cut along the negative real S axis, the inversion path can be distorted to run from $-\infty$ to 0 along the lower side of the cut and from 0 to $-\infty$ along the upper side. We make the substitution $s = -4c'x^2/h^2$ in the inversion integral, where x is real and nonnegative along the distorted inversion path, and note that

$$e^{st} = \exp(-4c't/h^2) = \exp[-(1 + r)x^2t/2t_d],$$

where

$$t_d = \frac{h^2}{8c'} + \frac{h^2}{8c}\left(\frac{N}{N'}\right)^2.$$

We find from numerical evaluations that t_d gives the time at which the pore pressure at the center of the fault has evolved approximately halfway toward its longer time limit of $\Delta p = -B\Delta\sigma_{kk}/3$. Hence

$$\frac{\Delta p'(t) - \Delta p}{\Delta p'(0^+) - \Delta p} = \frac{2\sqrt{r}}{\pi} \int_0^\infty \left(\frac{\sin(x)\exp[-(1+r)x^2 t/2t_d]}{x[\cos^2(x) + r\,\sin^2(x)]} \right) dx. \quad \text{(B2)}$$

The integral converges rapidly for $t > 0$ and can be evaluated by standard numerical integration schemes, although the number of numerical subdivisions becomes very large when r is either very large or small compared to unity. Fortunately, the limit cases can be treated separately. We find that when $r = 0$ (crust very much more permeable than the fault zone), the branch cut changes into a row of simple poles, giving

$$\frac{\Delta p'(t) - \Delta p}{\Delta p'(0^+) - \Delta p} = \frac{4}{\pi} \sum_{n=0}^\infty \frac{(-1)^n}{2n+1} \exp\left[-(2n+1)^2 \frac{\pi^2 t}{8t_d} \right] r = 0,$$

in which case $t_d = h^2/8c'$. That is just the classical Terzaghi one-dimensional consolidation solution for a layer which is freely drained at both sides.

[68] Also, either direct treatment or use of the substitution $y = x\sqrt{r}$ and taking the limit $r \to \infty$ (fault zone very much more permeable than crust) gives

$$\frac{\Delta p'(t) - \Delta p}{\Delta p'(0^+) - \Delta p} = \frac{2}{\pi} \int_0^\infty \left(\frac{\exp(-y^2 t/2t_d)}{1 + y^2} \right) dy \qquad r = \infty,$$

in which case,

$$t_d = \frac{h^2}{8c} \left(\frac{N}{N'} \right)^2.$$

The above expressions have been plotted in Figure 7 for various values of r on short and long timescales.

References

Beeler, N. M., R. W. Simpson, D. A. Lockner, and S. H. Hickman, Pore fluid pressure, apparent friction and Coulomb failure, *J. Geophys. Res.*, 105, 25,533–25,554, 2000.

Belardinelli, M. E., M. Cocco, O. Coutant, and F. Cotton, Redistribution of dynamic stress during coseismic ruptures: Evidence for fault interaction and earthquake triggering, *J. Geophys. Res.*, 104, 14,925–14,945, 1999.

Biot, M. A., General theory of three-dimensional consolidation, *Appl. Phys.*, 12, 155–164, 1941.

Biot, M. A., General solutions of the equations of elasticity and consolidation for a porous material, *J. Appl. Mech.*, 78, 91–98, 1956.

Byerlee, J. D., The change in orientation of subsidiary shears near faults containing pore fluid under high pressure, *Tectonophysics*, 211, 295–303, 1992.

Cocco, M., C. Nostro, and G. Ekstrom, Static stress changes and fault interaction during the 1997 Umbria-Marche earthquake sequence, *J. Seismol.*, 4, 501–516, 2000.

Cotton, F., and O. Coutant, Dynamic stress variations due to shear faulting in a plane-layered medium, *Geophys. J. Int.*, 128, 676–688, 1997.

Eberhart-Phillips, D., and A. J. Michael, Three-dimensional velocity structure, seismicity, and fault structure in the Parkfield region, central California, *J. Geophys. Res.*, 98, 15,737–15,758, 1993.

Eberhart-Phillips, D., and M. Reyners, Plate interface properties in the northeast Hikurangi subduction zone, New Zealand, from converted seismic waves, *Geophys. Res. Lett.*, 26, 2565–2568, 1999.

Green, D. H., and H. F. Wang, Fluid pressure response to undrained compression in saturated sedimentary rock, *Geophysics*, 51, 948–956, 1986.

Harris, R. A., Introduction to special section: Stress triggers, stress shadows, and implications for seismic hazard, *J. Geophys. Res.*, 103, 24,347–24,358, 1998.

Harris, R. A., and S. M. Day, Dynamics of fault interaction: parallel strike-slip faults, *J. Geophys. Res.*, 98, 4461–4472, 1993.

Harris, R. A., and R. W. Simpson, Changes in static stress on southern California faults after the 1992 Landers earthquake, *Nature*, 360, 251–254, 1992.

Hart, D. J., Laboratory measurements of a complete set of poroelastic moduli for Berea sandstone and Indiana limestone, M. S. thesis, 44 pp., Univ. of Wis., Madison, 1994.

Hill, D. P., et al., Seismicity remotely triggered by the magnitude 7.3 Landers, California, earthquake, *Science*, 260, 1617–1623, 1993.

Hudnut, K. W., L. Seeber, and J. Pacheco, Cross-fault triggering in the November 1987 Superstition Hills earthquake sequence, southern California, *Geophys. Res. Lett.*, 16, 199–202, 1989.

Johnson, P. A., and T. V. McEvilly, Parkfield seismicity: Fluid driven?, *J. Geophys. Res.*, 100, 12,937–12,950, 1995.

King, G. C. P., and M. Cocco, Fault interaction by elastic stress changes: New clues from earthquake sequences, *Adv. Geophys.*, 44, 1–38, 2000.

King, G. C. P., and R. Muir-Wood, The impact of earthquakes on fluids in the crust, *Ann. Geofis.*, XXXVII(6), 1453–1460, 1994.

King, G. C. P., R. S. Stein, and J. Lin, Static stress changes and the triggering of earthquakes, *Bull. Seismol. Soc. Am.*, 84, 935–953, 1994.

Kuempel, H. J., Poroelasticity: Parameters reviewed, *Geophys. J. Int.*, 105, 783–799, 1991.

Leary, P. C., Y. G. Li, and K. Aki, Observation and modelling of fault-zone fracture seismic anisotropy, I, *P*, *SV* and *SH* travel times, *Geophys. J. Astron. Soc.*, 91, 461–484, 1987.

Lees, J. M., Tomographic *P*-wave velocity images of the Loma Prieta earthquake asperity, *Geophys. Res. Lett.*, 17, 1433–1436, 1990.

Lees, J. M., and C. E. Nicholson, Three-dimensional tomography of the 1992 southern California earthquake sequence, *Geology*, 21, 387–390, 1993.

Li, Y. G., and P. C. Leary, Fault zone trapped seismic waves, *Bull. Seismol. Soc. Am.*, 80, 1245–1271, 1990.

Li, Y. G., P. C. Leary, K. Aki, and P. Malin, Seismic trapped modes in the Oroville and San Andreas fault zones, *Science*, 249, 763–766, 1990.

Li, Y. G., J. Vidale, K. Aki, J. Marone, and W. K. Lee, Fine structure of the Landers fault zone: Segmentation and the rupture process, *Science*, 265, 367–380, 1994.

Mooney, W. D., and A. Ginzburg, Seismic measurements of the internal properties of fault zones, *Pure Appl. Geophys.*, 124, 141–157, 1986.

Noir, J., E. Jacques, S. Békri, P. M. Adler, P. Tapponnier, and G. C. P. King, Fluid flow triggered migration of events in the 1989 Dobi earthquake sequence of central Afar, *Geophys. Res. Lett.*, 24, 2335–2338, 1997.

Nostro, C., M. Cocco, and M. E. Belardinelli, Static stress changes in extensional regimes: An application to southern Apennines (Italy), *Bull. Seismol. Soc. Am.*, 87, 234–248, 1997.

Nur, A., and J. R. Booker, Aftershocks caused by pore fluid flow?, *Science*, 175, 885–887, 1972.

O'Connell, R. G., and B. Budiansky, Seismic velocities in dry and saturated cracked solids, *J. Geophys. Res.*, 79, 5412–5426, 1974.

Okada, Y. , Surface deformation due to shear and tensile faults in a half-space, *Bull. Seismol. Soc. Am.*, 75, 1135–1154, 1985.

Okada, Y., Internal deformation due to shear and tensile faults in a half-space, *Bull. Seismol. Soc. Am.*, 82, 1018–1040, 1992.

Parsons, T., R. S. Stein, R. W. Simpson, and P. Reasenberg, Stress sensitivity of fault seismicity: A comparison between limited-offset oblique and major strike-slip faults, *J. Geophys. Res.*, 104, 20,183–20,202, 1999.

Perfettini, H., R. Stein, R. Simpson, and M. Cocco, Stress transfer by the *M* = 5.3, 5.4 Lake Elsnam earthquakes to the Loma Prieta fault: Unclamping at the site of the peak 1989 slip, *J. Geophys. Res.*, 104, 20,169–20,182, 1999.

Rice, J. R., The mechanics of earthquake rupture, in *Physics of the Earth Interior*, edited by A. M. Dziewonski and E. Boschi, *Proc. Int. Sch. Phys. Enrico Fermi*, 78, 555–649, 1980.

Rice, J. R., Fault stress states, pore pressure distributions and the weakness of the San Andreas fault, in *Fault Mechanics and Transport Properties of Rock*, edited by B. Evans and T.-F. Wong, pp. 475–503, Academic, San Diego, Calif., 1992.

Rice, J. R., and M. P. Cleary, Some basic stress diffusion solutions for fluid-saturated elastic porous media with compressible constituents, *Rev. Geophys.*, 14, 227–241, 1976.

Roeloffs, E., Poroelastic techniques in the study of earthquake-related hydrologic phenomena, *Adv. Geophys.*, *37*, 135–195, 1996.

Roeloffs, E., Persistent water level changes in a well near Parkfield, California, due to local and distant earthquakes, *J. Geophys Res.*, *103*, 869–889, 1998.

Roeloffs, E., and E. G. Quilty, Water level and strain changes preceding and following the August 4, 1985, Kettleman Hills, California, earthquake, *Pure Appl. Geophys.*, *149*, 21–60, 1997.

Roeloffs, E., and J. W. Rudnicki, Coupled deformation diffusion effects on water level changes due to propagating creep events, *Pure Appl. Geophys.*, *122*, 560–582, 1985.

Scholz, C. H., *The Mechanics of Earthquakes and Faulting*, 439 pp., Cambridge Univ. Press, New York, 1990.

Segall, P., and J. R. Rice, Dilatancy, compaction, and slip instability of a fluid infiltrated fault, *J. Geophys. Res.*, *100*, 22,155–22,171, 1995.

Sibson, R. H., Crustal stress, faulting and fluid flow, in *Geofluids: Origin, Migration and Evolution of Fluids in Sedimentary Basins*, edited by J. Parnell, *Geol. Soc. Spec. Publ.*, *78*, 69–84, 1994.

Simpson, R. W., and P. A. Reasenberg, Earthquake-induced static stress changes on central California faults, in *The Loma Prieta, California Earthquake of October 17, 1989—Tectonic Processes and Models*, edited by R. W. Simpson, *U.S. Geol. Surv. Prof. Pap., 1550-F*, F55–F89, 1994.

Skempton, A. W., The pore pressure coefficients A and B, *Geotechnique*, *4*, 143–147, 1954.

Stein, R. S., The role of stress transfer in earthquake occurrence, *Nature*, *402*, 605–609, 1999.

Stein, R. S., G. C. P. King, and J. Lin, Change in failure stress on the southern San Andreas fault system caused by the 1992 magnitude = 7.4 Landers earthquake, *Science*, *258*, 1328–1332, 1992.

Thurber, C. S., W. Roecker, W. Ellsworth, Y. Chen, W. Lutter, and R. Sessions, Two-dimensional seismic image of the San Andreas fault in the northern Gabilan Range, central California: Evidence for fluids in the fault zone, *Geophys. Res. Lett.*, *24*, 1591–1594, 1997.

Wang, H. F., *Theory of Linear Poroelasticity*, Princeton Univ. Press, Princeton, N. J., 2000.

Zhao, D., and H. Kanamori, The 1992 Landers earthquake sequence: Earthquake occurrence and structural heterogeneities, *Geophys. Res. Lett.*, *20*, 1083–1086, 1993.

Zhao, D., and H. Kanamori, The 1994 Northridge earthquake: 3-D crustal structure in the rupture zone and its relation to the aftershock locations and mechanisms, *Geophys. Res. Lett.*, *22*, 763–766, 1995.

Zhao, D., and T. Mizuno, Crack density and saturation rate in the 1995 Kobe earthquake region, *Geophys. Res. Lett.*, *26*, 3213–3216, 1999.

Zhao, D., and H. Negishi, The 1995 Kobe earthquake: Seismic image of the source zone and its implications for the rupture nucleation, *J. Geophys. Res.*, *103*, 9967–9986, 1998.

Zhao, D., H. Kanamori, and H. Negishi, Tomography of the source area of the 1995 Kobe earthquake: Evidence for fluids at the hypocenter?, *Science*, *274*, 1891–1894, 1996.

———————————

M. Cocco, Istituto Nazionale di Geofisica e Vulcanologia, Via di Vigna Murata 605, I-00143 Rome, Italy. (cocco@ingv.it)

J. R. Rice, Engineering Sciences and Geophysics, Harvard University, 29 Oxford St, 224 Pierce Hall, Cambridge, MA 02138, USA. (rice@esag.harvard.edu)

ERRATA CORRIGE (this compilation: 4 October 2002)

1. James R. Rice's correct affiliation (first page, just below title) is:
Department of Earth and Planetary Sciences and Division of Engineering and Applied
Sciences, Harvard University, Cambridge, Massachusetts.

2. There is a mistake in the equation included in Figures 4 and 5 for the isotropic
poroelastic model. The correct equation is: $\Delta CFF = \Delta\tau + \mu(\Delta\sigma_n - B\Delta\sigma_{kk}/3)$. The
figures were computed with the proper sign and are correct; only that equation is
misprinted.

3. Paragraph [38], Equation (21) should be: $B_{ij} = 3\partial p([\sigma],m)/\partial\sigma_{ij}$ (correcting the
placement of the closing square bracket and eliminating the unnecessary curly brackets).

4. Paragraph [40], Equation (22) should be: $B_{ij} = 3\rho\partial\varepsilon_{ij}([\sigma],m)/\partial m$ (again, correcting the
placement of the closing square bracket and eliminating the unnecessary curly brackets).

5. End of paragraph [44]: The correct relation is: $\Delta p' = -B\Delta\sigma_{kk}/3$ (instead of
$\Delta p' \approx -\Delta\sigma_{kk}/3$).

6. Appendix A, Equation (A3): The expression following the last equal sign should be:

$$d\left(\frac{pm}{\rho} - \hat{\mu}m\right) + \hat{\mu}dm$$

7. Appendix B, paragraph [65]: The upper case P which appears between the two sets of
equations in that paragraph should instead be lower case p.

8. Appendix B, paragraph [65]: Last member of second set of equations has the lower
case deltas within both parentheses. All four such deltas should be the partial derivative
sign (δ should be replaced by ∂).

9. Appendix B, paragraph [66]: The first term on the right of the second equation has a
lower case delta in the numerator which should be an upper case delta (δ should be
replaced by Δ).

Correction to "Pore pressure and poroelasticity effects in Coulomb stress analysis of earthquake interactions" by Massimo Cocco and James R. Rice

Citation: Cocco, M., and J. R. Rice, Correction to "Pore pressure and poroelasticity effects in Coulomb stress analysis of earthquake interactions" by Massimo Cocco and James R. Rice, *J. Geophys. Res.*, *108*(B2), 2069, doi:10.1029/2002JB002319, 2003.

[1] In the paper "Pore pressure and poroelasticity effects in Coulomb stress analysis of earthquake interactions" by Massimo Cocco and James R. Rice (Journal of Geophysical Research, 107(B2), 2030, doi:10.1029/2000JB000138, 2002), there are several corrections as follows:

1. James R. Rice's correct affiliation (first page, just below title) should be Department of Earth and Planetary Sciences and Division of Engineering and Applied Sciences, Harvard University, Cambridge, Massachusetts.

2. There is a mistake in the equation included in Figures 4 and 5 for the isotropic poroelastic model. The correct equation is $\Delta\text{CFF} = \Delta\tau + \mu(\Delta\sigma_n - B\Delta\sigma_{kk}/3)$. The figures were computed with the proper sign and are correct, only the text is wrong.

3. Paragraph [38], Equation (21) should be $B_{ij} = 3\partial p([\sigma], m)/\partial\sigma_{ij}$ (correcting the placement of the closing bracket and eliminating the unnecessary curly brackets).

4. Paragraph [40], Equation (22) should be $B_{ij} = 3\rho\partial\varepsilon_{ij}([\sigma], m)/\partial m$ (again, correcting the placement of the closing bracket and eliminating the unnecessary curly brackets).

5. End of paragraph [44]: The correct relation is $\Delta p' = -B\Delta\sigma_{kk}/3$ (instead of $\Delta p \approx -\Delta\sigma_{kk}/3$).

6. Appendix A, equation (A3): The expression following the last equals sign should be $d\left(\frac{pm}{\rho} - \hat{\mu}m\right) + \hat{\mu}dm$.

7. Appendix B, paragraph [65]: The capital P that appears between the two sets of equations in that paragraph should instead be lowercase p.

8. Appendix B, paragraph [65]: Last member of second set of equations has the lower case deltas within both parentheses. All four such deltas should be the partial derivative sign (δ should be replaced by ∂).

9. Appendix B, paragraph [66]: The first term on the right of the second equation has a lowercase delta in the numerator which should be an capital delta (δ should be replaced by Δ).